N O T I C E

THIS DOCUMENT HAS BEEN REPRODUCED FROM MICROFICHE. ALTHOUGH IT IS RECOGNIZED THAT CERTAIN PORTIONS ARE ILLEGIBLE, IT IS BEING RELEASED IN THE INTEREST OF MAKING AVAILABLE AS MUCH INFORMATION AS POSSIBLE

NASA

Technical Memorandum 80731

SURVEY OF THE PLASMA ELECTRON ENVIRONMENT OF JUPITER: A VIEW FROM VOYAGER

J. D. SCUDDER, E. C. SITTLER JR.
AND H. S. BRIDGE

AUGUST 1980

A SURVEY OF THE PLASMA ELECTRON ENVIRONMENT OF JUPITER:

A VIEW FROM VOYAGER

by

J. D. Scudder

E. C. Sittler, Jr.

NASA/Goddard Space Flight Center

Laboratory for Extraterrestrial Physics

Greenbelt, MD 20771

and

H. S. Bridge

Center for Space Research

Massachusetts Institute of Technology

Cambridge, MA 02139

ABSTRACT

A survey of the plasma environment within Jupiter's bow shock is presented in terms of the in situ, calibrated electron plasma measurements made between 10 eV and 5.95 keV by the Voyager Plasma Science Experiment (PLS). These measurements have been analyzed and corrected for spacecraft potential variations; the data have been reduced to nearly model independent macroscopic parameters of the local electron density and temperature. The electron parameters are derived without reference to or internal calibration from the positive ion measurements made by the PLS experiment. Extensive statistical and direct comparisons with other determinations of the local plasma charge density clearly indicate that the analysis procedures used have successfully and routinely discriminated between spacecraft sheath and ambient plasmas. These statistical cross correlations have been performed over the density range of 10^{-3} to 2×10^{2}/cc. These data clearly define the bow shock, the magnetosheath (30-50 eV) the magnetosphere (10^{-2}/cc, 2-3 keV) as well as the periodic appearances of the plasma sheet which are illustrated to be routinely cooler than the surroundings. The proximity of the plasma sheet defines a regime in the magnetosphere where very cold electron plasma (as low as 50 eV) at 40 R_J can be seen in unexpected density enhancements. These plasma "spikes" in the density can often represent an order of magnitude enhancement above the ambient density and are correlated with diamagnetic depressions. These features have been seen at nearly all magnetic latitudes within the plasma sheet. The temperature within these spikes is lowered by similar factors indicating that the principal density enhancements are of cold plasma. The plasma sheet when traversed in the outer magnetosphere has a similar density and temperature morphology as

that seen in these "spikes". In all cases the plasma sheet crossing lasts for intervals commensurate with that defined by the diamagnetic depression in the simultaneously measured and displayed magnetic field. The electron temperatures in the plasma sheet in the outer and middle magnetosphere appear to have a positive radial gradient with jovicentric distance. The electron temperature is observed to be lower on the centrifugal side of the minimum magnetic field strength seen in each sheet, while the suprathermal electron density is enhanced symmetrically about the locally indicated magnetic equator. The electron distribution functions within the plasma sheet are markedly non-Maxwellian; during the density enhancement's of the plasma sheet the thermal sub-population is generally enhanced more than the suprathermal population. The suprathermal fraction of the electron density within the plasma sheet is an increasing function of jovicentric distance. Direct, in situ sampling of the electron plasma environment of Io's torus clearly illustrates that the system is demonstrably removed from local thermodynamic equilibrium; these measurements illustrate that between 5.5 and 8.9 R_J there are sizeable systematic variations of the macroscopic and microscopic parameters; there are at least three electron thermal regimes within the torus. These three regimes have mean electron energies in the outer, temperate, and inner torus of the order of 100, 10-40, and less than 5 eV, respectively. The distribution functions in these regimes are always non-Maxwellian with the suprathermal population an increasing fraction of the density and partial pressure with increasing distance from Jupiter. The common non-Maxwellian character of the electron torus plasma unequivocally implies that the electrons and ions cannot locally have the same temperature if binary Coulomb collisions are the only scattering present in the plasma torus. The direct in situ torus electron spectra are

shown to be compatible with a number of indirect assessments of the electron state in the torus including observations of plasma hiss, whistler Landau damping, gyro-harmonic emissions, possible asymmetric sink for collisional ionization of sodium, and capacity to ionize sulfur whose presence is implied by the optical and EUV measurements.

It is also suggested that the Io plasma torus is the limiting form of the plasma sheet, possibly being its complete direct source, since a progression in the fractional number in the cold, or thermal number density is clear: this fraction is 0.999 in the inner torus, but only 0.5 in the plasma sheet at 40 R_J. We have tentatively concluded that the radial temperature profile within the plasma sheet is caused by the intermixing of two different electron populations that probably have different temporal histories and spatial paths to their local observation. The cool plasma source of the plasma sheet and spikes is probably the Io plasma torus and arrives in the plasma sheet as a result of flux tube interchange motions or other generalized transport which can be accomplished without diverting the plasma from the centrifugal equator. The hot suprathermal populations in the plasma sheet have most recently come from the sparse, hot mid-latitude "bath" of electrons which were directly observed juxtaposed to the plasma sheet. As the cool plasma is diluted by filling an increasing volume as it undergoes radial expansion, the outer hot bath of electrons can increasingly dominate until at sufficient radial distance the sheet per se does not exist anymore.

I. INTRODUCTION

1) Pioneer Data

Before the Voyager spacecraft encounters with Jupiter in 1979 the plasma within the Jovian magnetosphere was principally defined by the in situ measurements of fluxes of ions and electrons capable of exciting solid state telescopes and Geiger tubes with lowest energy thresholds of 61 and 16 keV, respectively for ions and electrons. Particle fluxes in these energy ranges clearly showed dramatic enhancements over the nearby interplanetary level, periodic modulations within the magnetosphere, and effects of satellite sweeping--Van Allen et al. (1974a,b), Van Allen et al. (1975), Fillius and McIlwain (1974), Fillius et al. (1975), Trainor et al. (1974), Trainor et al. (1975), Simpson et al. (1974), McKibben and Simpson (1974), and Simpson et al. (1975).

Lower energy plasma measurements were also attempted using electrostatic analyzers with encounter mode energy ranges of $100-E_i-4800$ eV and $1-E_e-500$ eV for the ions and electrons, respectively. Although these instruments were not designed for the harsh radiation environments within the magnetosphere, after performing a difficult subtraction of the penetrating radiation fluxes, Frank et al. (1976) reported results of the positive ion measurements which were assumed to be protons. These authors reported ion temperatures ranging between 100-1000 eV and substantial density enhancements at the orbital positions of Europa, Io, and Almathea, with peak densities in the Io vicinity of approximately 50/cc. They suggested the presence of a plasmasphere within a plasmapause near 6 R_J and that the observed plasma originated from Jupiter's ionosphere. Siscoe and Chen (1976-1977) came to a different conclusion, suggesting that the density enhancement near Io's orbit indicated that it was the source of

the plasma Frank et al. reported. Neugebauer and Eviatar (1976) came to a
similar conclusion as Siscoe and Chen; they also suggested a
reinterpretation of the Pioneer measurements concluding that the observed
fluxes were probably heavy ions, especially in view of the presence of
other heavy neutral and ionized material that had been inferred from the
optical data (NaI Brown (1973), and SII Kupo et al. (1976)) and that the
expected corotational energy for protons (16.3 eV) at Io's orbit was
considerably below Frank et al's. 100 eV low energy window.

The interpretation of the thermal electrons by Intriligator and Wolfe
(1974), Intriligator and Wolfe (1976), and Intriligator and Wolfe (1977)
from the electrostatic analyzers were largely qualitative owing to the
variable and substantial spacecraft potentials apparently experienced.
However, in the presence of such difficulties, the inferences ($n_e \sim 1/cc$,
$T_e \sim 4$ eV, no 10-hour modulation or radial variation) that were drawn from
the electron measurements were questioned by Grard et al. (1977), who
suggested that the analyzed measurements pertained more to the spacecraft
sheath of trapped photoelectrons and secondary electrons rather than to the
ambient plasma population of the magnetosphere proper.

2) Optical Inferences

The implications of various optical measurements in the
intervening time between Pioneer and Voyager encounters had further defined
the astrophysical setting of the plasma near the orbit of Io. In 1973
Brown reported and confirmed (Brown and Chaffee (1974)) the detection of
neutral sodium emissions from the vicinity of Io. Trafton et al. (1974)
established that the resonantly scattered sunlight was the probable
excitation mechanism and that the neutral sodium emission came from a
distributed source, rather than from a localized atmosphere. These authors

also concluded that the neutral sodium "cloud" was incomplete in System III

longitude, and usually, but not always, stronger on the Jovian side within

Io's orbital plane, and weakened (Trafton and Macy (1975) and Trafton

(1977)) by the passage of Io through the magnetic equator. Trafton also

discovered and confirmed (1977) the trace presence of neutral potassium in

Io's cloud. Trafton and coworkers suggested that the modulation of the

neutral sodium emission was caused by impact ionization by the plasma

(electrons) confined to the magnetic equator. Carlson et al. (1975) had

earlier correctly suggested, based on the Pioneer plasma quantities, that

impact ionization by thermal electrons of neutrals within Io's torus would

be the dominant loss mechanism. By independent arguments Eviatar et al.

(1976) reached a similar conclusion. The in situ ultraviolet measurements

conducted on the Pioneer spacecraft were interpreted by Carlson and Judge

(1974) to imply the existence of an incomplete neutral hydrogen torus

concentric with Io's orbit. (The measurements have recently been

reinterpreted by Mekler and Eviatar (1980) as emissions of sulfur and

oxygen ions.) The inference of neutral species with ionization potentials

of 5.3 and 13.6 eV within the radiation belts of Jupiter put some

degenerate but instructive limits on the probable combinations of density

and temperatures of the plasma environments that would allow neutrals to

remain unionized. Before the Voyager encounters the sodium emissions were

confirmed by several independent observers; they were documented: 1) to be

a more or less permanent feature of the inner Jovian magnetosphere (Trafton

and Macy (1975), Brown et al. (1975), Mekler and Eviatar (1978), Trafton

(1977); 2) to possess substantial temporal variations (actual and apparent)

(Trafton and Macy (1975), Brown and Yung (1976), Trafton (1977), Murcray

and Goody (1978) and Merkler and Eviatar (1978, 1980)); 3) to be

concentrated when present on the Jupiter side, or inner edge of Io's orbit. Some Keplerian studies by Smyth and McElroy (1977) have also discussed the likely locations of the escaping neutral sodium from Io's surface.

In 1976 evidence for ionized sodium plasma was announced [Eviatar et al. (1976)] and Kupo, Mekler and Eviatar reported the emission features in Io's spectrum which they assigned to the deexcitation transition of collisionally populated excited states of singly ionized sulfur, which has an ionization potential of 10.4 eV. The ionized sulphur emission appeared to be strongly anti-correlated with the neutral sodium emission, which led these authors also to infer that collisions, which could ionize and excite the sulfur, would also lead to the demise of the neutral sodium with the corresponding reduction in the resonantly scattered sunlight. An upper limit on the density in the torus was suggested by Kupo et al. (1976). Citing classical methods for studying the electron environments of gaseous nebulae, Brown (1976) suggested that the emission features reported by Kupo et al. could be used as a remote indicator of the electron density and the temperature; the values he determined were

$$\log n_e = 3.5 \pm 0.5 \text{ and } \log T_e = 4.4 \pm 0.6 ^\circ K.$$

By relaxing Brown's approximations, Mekler et al. (1977) suggested n_e ∿ 500 and T_e ∿ 10 eV were more appropriate. Mekler and Eviatar (1978) used a large catalogue of observations of the anti-correlations of NaI and SII emissions to infer probable ranges of the electron densities between 1974 and 1977 to be 50-900/cc.

3) Voyager Inferences of Electron Properties

Using the Voyager data there have been a variety of additional inferences of the properties of the electrons within Jupiter's magnetosphere. In varying degrees these measurements require certain

assumptions about 1) the distributed plasma volume sampled in the case of integral or line of sight measurements or 2) the inferred phase space distribution of electrons or 3) arguments by analogy with the earth's plasma properties. The principal tools (inferences) in these efforts have been the rich variety of EUV emissions reported and discussed by Broadfoot et al. (1979), Sandel et al. (1979) and Shemansky (1980) (apparent line of sight average electron temperature ($\sim$ 10 eV) and densities), radio propagation characteristics during the Io torus occultation of the Voyager spacecraft (average electron density in torus column) by Eshelmann et al. (1979), the gyroharmonic electrostatic emissions (local "cold" n_e) by Warwick et al. (1979a), and assignments of the upper hybrid "line" (n_e) by Gurnett et al. (1979) vs. Warwick et al. (1979b). Of all these inferences those determined by the cutoff of the continuum plasma radiation as determined by the broadband data discussed by Scarf et al. (1979), Barbosa et al. (1979), Gurnett et al. (1980) and in detail by Gurnett et al. (1981) are most directly related to the local total electron density at the spacecraft. Other electron properties, such as the apparent "torus average" electron temperature (if it were Maxwellian) was inferred from the frequency dependence of damping of the whistler mode radiation by Menietti and Gurnett (1980); densities of keV electrons were inferred by Coroniti et al. (1980) within Io's torus to support the hiss noise reported there; non-thermal electron distribution functions were invoked by Warwick et al. (1979a) and Birmingham et al. (1981) for the Io torus measurements, by Barbosa et al. (1979) and Kurth et al. (1980) during the crossing of the magnetic equator inside of 23 R_J in order to understand the gyroharmonic electrostatic emissions observed as in analogy to that seen at earth. Recently Strobel and Davis (1980) have also suggested that a non-thermal

distribution of electrons is required within the plasma torus of Jupiter to understand the line intensities and features observed by the EUV measurements.

4) Voyager In Situ Electron Measurements

This paper documents the first quantitative definition of the electron thermal plasma environment within Jupiter's magnetosphere in terms of the plasma electrons that are directly observed by the Plasma Science Experiment (PLS). However, local time morphology is not addressed in the current survey. This experiment has been fully described by Bridge et al. (1977) and is the first low energy plasma instrument designed specifically to operate in the solar wind and within the magnetosphere of Jupiter. Initial Jupiter encounter PLS results, primarily of ions, have been reported by Bridge et al. (1979a), Bridge et al. (1979b), McNutt et al. (1979), Sullivan and Bagenal (1979), Bagenal et al. (1980), Belcher et al. (1980), and McNutt et al. (1981).

The electron populations between 10 eV and 5.95 keV have been routinely sampled in the solar wind by the Plasma Science Experiment since the instrument turn-on, have been successfully analyzed, and have been reported in the literature (Sittler et al. (1979), and Sittler and Scudder (1980)). As will become clear in the analysis section of this paper, our quantitative encounter analysis makes detailed use of the average properties of the spacecraft surface that have been gleaned from an extensive cruise data reduction that has only been recently completed. In a forthcoming paper results from this cruise analysis will be given, including a comprehensive discussion of the analysis procedures used which are only cursorily discussed in this paper. This order of the data reduction was required in order to preserve the independence of the direct

electron analysis from the parallel and ambiguous determinations that are implicit in E/Z measurements of the ionic phase density (PLS and LECP). In order to appreciate the great value of the complementary electron measurements in defining the magnetosphere of Jupiter on the Voyager mission, it should be realized that there is no unique way of assigning the partition by number of the ionic plasma composition below $E_0 \approx 200$ keV. The ionic discrimination above this energy is determined by solid state methods as reported by Krimigis et al. (1979a,b) and Vogt et al. (1979). Varied heavy ion composition has been clearly shown above E_0 as well as in the EUV emission features that have already been alluded to. Since the direct, local low energy ($E < E_0$) ionic measurements are only resolved with respect to energy per unit charge, there is a certain subjectivity involved in assigning this much of the flux in a given channel to species X and this fraction from species Y, ... which per chance have the same energy per unit charge. This degeneracy has until now been approached in two ways (Belcher et al., 1980; Krimigis et al., 1979a). The first of these approaches (PLS) assumes that multiple species, if present, should have a common corotational bulk motion, and examines the patterns in the determinations on this assumption that are seen in A/Z implied; in particular, when individual peaks are not resolved, the species present are assumed to be similar to that most recently seen, with the smearing of the fluxes attributed to an enhanced thermal speed for these populations. The LECP team's approach to the analysis of their measurements assumes that the composition directly measured at $E > E_0$ is the appropriate compositional distribution of the lower energies ($E < E_0$) where the phase space densities are in principle degenerately mixed. Studying the constraint of local gross charge neutrality with the availability of the electron density can

help to decipher the convolutions over species present in the raw ion
fluxes for energies below E_o.

The complications of blended ionic phase densities are not present in
the energy per unit charge fluxes of negatively charged fluxes, except in
those unusually cool plasmas where stable anions can reside with
significant lifetimes against breakup: anions usually have very low binding
energies ($E_B < 1$ eV) relative to even the lowest quantitative electron
temperature that have been directly determined within Jupiter's
magnetosphere. However, an exhaustive list of anions (and their binding
energies) that could result from the demise of neutral volcanic gases is
not available, and there has been a recent suggestion [Cheng (1980)] that
there should be a significant number of anions within the plasma torus. By
the usual pick-up arguments for newborn (an)ions, these heavy anions if
dominant by number would have nearly the corotational bulk and thermal
energy, making them conspicuous transonic peaks in the negative flux
currents. A search for such distributions is in progress; however, for the
data discussed in this paper these signatures are not discernible nor
likely to be present.

In view of the controversy surrounding the interpretation of similar
energy range measurements on the Pioneer spacecraft, the initial sections
of this paper are devoted to validating the measurement and analysis
procedures. This is done by comparing quantities determined solely from
the in situ PLS electron measurements with other quantities that are
independently measured and that are theoretically expected to be
comparable. These comparisons are of three types: 1) direct comparisons
of the PLS electron densities with those determined from the continuum
cut-off as reported by Gurnett et al. (1981); 2) pressure balance studies

across interplanetary and magnetopause discontinuities; and 3) internal comparison between the electron charge density inferred at NASA/GSFC from the PLS electron fluxes, with the ion charge density determined independently by our MIT colleagues from the positive ion fluxes (cf. McNutt et al. (1981). These comparisons indicate that our electron analysis procedures are routinely compatible with the theoretical requirement of charge neutrality of the plasma on spatial scales larger than the debye length. These comparisons span four and one-half orders of magnitude in ambient density ($5 \times 10^{-3} - 2 \times 10^2$/cc) and clearly indicate that routine discrimination between ambient electron population and those characteristic of the spacecraft sheath has been accomplished even in the rarefied distant magnetosphere. These comparisons span regimes between the magnetopause and closest approach on both spacecraft, including outer magnetosphere, middle magnetosphere and within the plasma torus. Having validated our basic measurement and analysis procedures we will highlight the regimes suggested within the magnetosphere as defined by the non-relativistic electrons and discuss their relationship to the growing body of inferences from the indirect measurements referred to above as well as their relationship to the ion morphology reported by PLS and LECP Krimigis et al., 1979a,b.

II. PLS ELECTRON INSTRUMENT

The direct sampling of the ambient plasma electrons between 10 eV and 5.95 keV was obtained on the Voyager spacecraft by a cylindrical, potential modulated Faraday cup which is usually oriented nearly orthogonal to the solar direction on the ordinarily attitude stabilized spacecraft. The design of the cup and its relation to the other PLS sensors is discussed extensively in Bridge et al. (1977). The currents transmitted to the earth

are determined by ac synchronous current detection and do not contain dc background contributions that arise from penetrating (unmodulated) radiation. The field of view of the cup (variously referred to as the side or "D" cup) is ±45° and the response is cylindrically symmetric about the normal to the collector [Binsack (1966); Sittler (1978); Olbert, private communication (1980)]. The fluxes measured by the instrument are essentially differential in the normal component of the electron speed to which it is tuned; however the detector's response is integral with regards to the velocity components transverse to the cup normal. (These concepts are discussed in detail in Sittler (1978); Sittler et al. (1979).) As discussed extensively in Sittler and Scudder (1981), the phase space distribution function along the cup normal is retrievable in spite of the integral character of the detector's transverse response, so long as the velocity windows Δv are everywhere small compared to the magnitude of the reciprocal of the local logarithmic derivative of the distribution function with respect to speed. Loosely, this condition is equivalent to saying that the velocity windows are narrow with respect to the thermal spread, w, of the electron distribution. At low energies (below 140 eV), the speed windows are of the order of 300 km/s, whereas even a very cold electron plasma with a 2 eV temperature has a thermal speed of 1000 km/s; in the keV regime of electron temperatures, the thermal speeds are on the order of 20,000 km/s, and the instrument window widths Δv ∿ 4000 km/sec; therefore, this condition of differential measurement is routinely met so long as the plasma-spacecraft floating potential is not excessively high. As outlined below we explicitly determine the self-consistent floating spacecraft potential and show that this latter concern is not a serious problem for the Voyager vehicles.

It should be noted that our present analysis has neglected the corrections resulting from secondary electrons emitted from the collector plate of the cup and not successfully returned to it by the supressor grid. However, a preliminary study indicates that this effect will result in an underestimate of the electron density by no more than 10% for T_e < 100 eV, and no more than 30% for T_e > 100 eV. Such corrections will be made in the near future.

III. MACROSCOPIC ELECTRON PARAMETERS

Once the distribution function f(v) is determined along the cup normal estimates of the electron density and temperature can be estimated by the following quadratures:

$$n_e \approx 4\pi \int_0^\infty f(v_d) v_d^2 dv \tag{1}$$

$$T_e \approx 4\pi \int_0^\infty f(v_d)\, 1/2\, m_e v_d^2 v_d^2 dv_d /(3/2n\, k_B) \tag{2}$$

where v_d, defined by

$$v_d = \sqrt{v_o^2 - 2|e|\phi_{SC}/m_e}, \tag{3}$$

is the speed that an electron collected at the spacecraft with an observed speed v_o would have had prior to dropping through a spacecraft potential $e\phi_{SC}$. The factor of 4π embodies the assumption that the phase space sampled in the direction of the cup normal is representative of 4π strd. The nature of the isotropy assumption in the spacecraft frame implies that the electron plasma pressure is approximated as isotropic and that the excellent approximation that the plasma flow velocity, U, scaled by the electron thermal speed, w, is small. For our calculations we have assumed U/w = 0. The large thermal speed of electrons (T = 2 eV implies w ᷈ 1000

km/s!) makes this latter approximation excellent nearly everywhere in astrophysical plasmas, unless the odd moments of the plasma such as bulk velocity or heat flux are themselves being determined (cf. Ogilvie and Scudder, 1978). In the above approximation one can show using Liouville's theorem that the phase density $f(v_d) \approx f(v_0)$, (i.e., implementing a simple energy shift correction), so long as the sensor does not sample an appreciable fraction of electron trajectories passing closer than 45° to the spacecraft skin. For the Voyager PLS instrument this condition is always met (Sittler, 1978). The extent of good correlation of the derived quantities in the presence of these assumptions will be commented on below.

The limits of integration defined above are those of the kinetic definition of density and temperature. Usually the distribution function $f(v_d)$ is not sampled directly at or near zero v_d by the electron experiment with its low energy threshold of 10 eV. We attempt to correct to first order for the low energy variation of $f(v_d)$ below our threshold by extrapolating the Gaussian tendency indicated by the first few channels above our energy threshold. In addition, the integrands go to zero in this vicinity as v_d^2 and v_d^4 assuming that f is not varying too rapidly below 10 eV relative to that indicated by the channels above 10 eV. These two effects imply that small contributions to the integrals are made below 10 eV except in the circumstance that the low energy Gaussian "temperature" is much colder than 10 eV, or the electrostatic spacecraft plasma potential is negative by an amount comparable to the local plasma electron temperature. This effect yields uncertainties rarely larger than 5%, when T_e is greater than 5 eV, which is the situation in most of the magnetosphere. The actual observations do not extend to infinite energy, either. However, the 6 keV upper energy limit is generally large enough to

estimate the trend of $f(v)$ near the upper threshold. This trend plus the knowledge that $f(v)$ must go to zero faster than $1/v^2$ in order that the density exist, allow estimates to be made for the unmeasured density and the fractional imprecision caused. Because the characteristic energy as reflected in T_e determined in this way is rarely over 2-3 keV, these fractional corrections to the density from $E > 6$ keV electrons are only 10% when the temperature is this high and much smaller if the characteristic T_e is smaller.

It should be reemphasized that this approach has attempted to quantify the electron properties as a kinetic gas, deriving densities and temperatures that do not refer to a particular energy range but to the gas as a whole. In this sense the derived temperatures represent evaluations of the mean random energy possessed by the gas; this quantity, as is well known, agrees with a similar value determined by fitting a Gaussian (Maxwellian) to some energy sub-interval, provided the distribution is known to be Maxwellian in the measured energy range and over those energies which dominate the density and temperature. This fortunate circumstance is rarely encountered in astrophysical plasmas; the observed distributions generally possess suprathermal tails. This point has recently been reemphasized in connection with the observed ions at Jupiter by Belcher et al. (1980). Regardless of the non-thermal tails, the energy densities of all the particles do act as the gas pressure; in this sense the numerically determined quantities outlined above do characterize the electron density and pressure, provided it can be documented that 1) all the ambient electron density is accounted for and 2) that the extrapolation above 6 keV makes a small contribution to the pressure integral.

The remaining particular in carrying out these quadratures, is the

determination of the spacecraft floating potential, ϕ_{SC}, as a function of time during the encounter. In theory and practice this is not a constant quantity, and the ability to infer how this quantity varies, is synonymous with the ability to exclude from the analysis those currents to the detector that arise from trapped photoelectrons and secondary electrons which encircle the spacecraft in a sheath. This quantity is determined with the assistance of the detailed analysis and comparison of the solar wind cruise analysis that will be briefly discussed in the next section.

IV. SPACECRAFT POTENTIAL AND RETURN CURRENT RELATION

The spacecraft potential is dynamically determined in two different ways depending on the availability of ion charge density constraints.

1. Cruise Phase: Potential Determination

During the cruise portion of the Voyager mission the floating potential is determined in an iterative way so that by its assignment, the integrated, or moment definition of the measured solar wind electron charge density equals that independently determined for the ions. (In the supersonic solar wind, the ion number density for the protons and alphas are very accurately determined from the forward Faraday cups of the PLS experiment (cf. Bridge et al. (1977)). The first approximation to the size of this potential can be easily determined as

$$e\phi_{SC}^{(0)} = -kT_e \ln \left[\frac{n_p + 2n_\alpha}{n_-^*} \right]$$

where n_p and n_α are the proton and alpha number densities and n_-^* is the apparent electron density under the assumption that $\phi_{SC} = 0$. Subsequent iterations are performed until $n_e(\phi^{(n)}) = n_p + 2n_\alpha$.

As an experimental by-product of this procedure, we can determine the plasma return current density, $J(\phi_{SC}, r, t)$ which is approximately the

electron thermal flux. This return current and associated floating

potential $\phi_{SC}(r,t)$ were determined by enforcing charge neutrality during

the cruise portion of the mission. Significant variability in $\phi_{SC}(r,t)$

takes place during cruise and allows a statistical determination of the

relation between the return current and the floating potential that is used

as a "calibration curve" for the spacecraft-plasma interaction when the

positive ion charge density may be unknown, imprecise, or highly model

dependent.

2. Cruise Phase: Return Current Relation Construction

The floating potential of the spacecraft at a fixed position in

sunlight is determined parametrically by the ambient plasma return current

that is intercepted by the spacecraft surface. This potential floats to a

value so that the intercepted ambient plasma current, $J_{return}(\phi_{SC},r,t)$ in

the presence of the potential ϕ_{SC} is precisely balanced by the

photoelectron current that can escape from the spacecraft to infinity in

the same electrostatic potential. Thus a potential ϕ_{SC} is established so

that

$$J_{return}(\phi_{SC},r,t)\, A_{SC} = J_{photo}\, A_{sunlit} \qquad (4)$$

where A_{SC} and A_{sunlit} are the receiving and illuminated surface areas on

the spacecraft and where

$$J_{return}(\phi_{SC},r,t) \simeq \int_{|V_{\phi SC}|}^{\infty} f_e(\vec{V}_o)\, \vec{V}_o \cdot \hat{n} d^3 V_o,$$

where $\vec{V}_o$ is the observed velocity, $V_{\phi SC} = (2|e|\phi_{SC}/m_e)^{1/2}$, and $\hat{n}$ is the cup

(spacecraft) normal. Since the escaping photoelectron current is larger

for smaller ϕ_{SC}, it should be clear that the floating potential and plasma

return current should be anti-correlated. Because of the stream dynamics

and time variability of the solar wind plasma, the return current, and correspondingly the spacecraft potential, will vary in time for fixed radial distance. In addition, because the spacecraft is moving away from the sun, the UV flux and corresponding reservoir of available photoelectrons in the surrounding sheath will vary with a $1/r^2$ dependence. Therefore, the observed return current at r will scale like $(r_0/r)^2$ relative to some reference point r_0 assuming other conditions remain unchanged. To put it another way, for fixed spacecraft potential, the photocurrent leaving the spacecraft will vary like $1/r^2$.

In Figure 1 we have plotted the empirical "return current relation" derived from our cruise analysis [Sittler and Scudder (1981)]. The return current plotted along the ordinate is normalized to 1 AU by the following relation:

$$J_R \ (1 \ AU) = J_R \ (obs) \left[\frac{r_{obs}}{r_{AU}} \right]^2$$

while the abscissa is the spacecraft potential. Above 0.1 volts we find this relation is well fit with a power law of negative slope with power law index -2.0 ± 0.08. The data points have been computed by binning over 5700 hourly averages within bins of equal width along the best fit line [cf. Sittler and Scudder (1980), where similiar binning and fitting procedures are used]. Errors in the mean of the individual points are smaller than the plotting symbols. The solid curve indicates this fit to the data for potentials greater than 0.1v. The turn over at lower potentials results from a saturation of the photoelectron current at zero volts where all the available photoelectrons have escaped to infinity; the placement of this dashed curve segment is approximately indicated and will be defined experimentally by future work. The slope and magnitude of the power law

portion of this curve are consistent with theoretical and observational

expectations at 1 AU (see Reasoner and Burke (1972)). This empirically

constructed curve, which we have called the "return current relation",

represents a statistical, empirical synthesis of the equilibrium properties

of the plasma/Voyager spacecraft surface interaction in sunlight and can be

used as a calibration curve within Jupiter's magnetophere and in the deep

solar wind.

3. Encounter Phase: Using the Cruise Return Current Relation

With the return current relation developed during cruise, the analysis

of the electron data taken within Jupiter's bow shock is completely

independent of the ion measurements. Our procedure is to assume a fi.st

guess of the floating potential, $\phi_{SC}^{(1)}$, on the order of the most prcbable

energy of the data under consideration; under this assumption the return

current to the spacecraft implied by the measurements of electrons with

observed energies $E > e\phi_{SC}^{(1)}$ is determined. This current, parametric in

the assumed potential, is then compared with the equilibrium return current

expected at potential $\phi_{SC}^{(1)}$ on the basis of the "return current relation"

derived from the cruise data. The potential is then iterated until the

observed return current and potential assignment $\phi_{SC}^{(n)}$, are compatible

with the statistical, cruise generated calibration curve shown in Figure 1.

This potential is then used in the velocity space transformations necessary

to evaluate the moment density and temperature integrals (cf. eqtns.

(1-3)).

4. Encounter Phase: Return Current Relation Complications:

Secondary Production:

The return current relation discussed previously was generated under

interplanetary conditions when the effects of secondary electron production

in the spacecraft plasma balance were not very important. Within Jupiter's magnetosphere where the energetic particle radiation is orders of magnitude higher, the spacecraft plasma interaction is further complicated by the potentially significant reduction in the plasma current as a result of escaping secondary electrons. Thus the plasma return current is more correctly the primary current less the escaping secondary current. Several mitigating factors make this effect less important than one would ordinarily surmise. They are: 1) when the electrons are sparse, $n_e \sim 10^{-3}$/cc, they are hot $T_e \sim$ keV; 2) when they are denser, $n_e \gtrsim 10^{-1}$/cc, they are colder $T_e \lesssim 100$ eV; and 3) the non-linear dependence of the spacecraft potential upon the plasma return current (see Figure 1).

In the outer magnetosphere where return currents are low and electron temperatures $\sim$ keV the spacecraft floating potential Φ_{SC} may be on the order of tens of volts (cf. Figure 3). For electron energies greater than a few hundred eV, secondary yields may get over one, and dominate the photocurrent at these high spacecraft potentials. (Note that almost all secondary electrons are due to primary <u>electrons</u> which have higher yields and larger thermal speeds than ions). Since almost all secondaries have energies $\lesssim 20$ eV [cf. Bruining (1954)], they will contribute only to the photo-current for $\Phi_{SC} \lesssim 20$ volts, since for $\Phi_{SC} > 20$ volts all secondaries are returned to the spacecraft. Therefore, in such regions we may underestimate Φ_{SC} by no more than $\delta\Phi_{SC} \sim 10$ volts. Since electron temperatures are $\sim$ keV in these regions, negligible corrections ($\sim 1\%$) to our density estimates results, since this error scales as $\exp(-e\delta\Phi_{SC}/kT_e)$.

When the electrons are colder, the density and return currents are much higher so that in these regions the spacecraft potentials are $\lesssim 1$ volt. Because of the colder temperatures ($T_e < 100$ eV) most of the primary

electrons have yields $\lesssim$ 50%. This means we may overestimate the return current (primaries minus secondaries) by no more than a factor of 2 and correspondingly underestimate the spacecraft potential by no more than a volt or two (refer to Figure 1). One then finds that corrections to the electron density for $\phi_{SC} > 0$ are no more than 10% for the worst case. The only regions where such corrections may be important are those where the spacecraft goes negative, inside the denser cooler regions of Io's plasma torus and within shadow. Under such conditions, the return current relation as shown in Figure 1 is very flat, so that changes in the spacecraft potential $\sim kT_e$ is required in order to counter any increases in the return current. Therefore, a factor of two error in the return current will produce a similar error in the electron density. In future analysis, secondary electron corrections are planned where its major impact will be within Io's torus and regions where the spacecraft goes into shadow. Albedo

As Jupiter is approached the illuminated area of the spacecraft is increased since the nearby presence of the planet acts like a solar UV mirror. This effect can be very important in the negative potential regime of Figure 1, where a very small change in the emitting sunlit area (cf. eqtn. 4) and therefore photocurrent (not photocurrent density), which equals the plasma return current, dictates a very large change in the floating potential relative to kT_e to remain on the return current relation. These corrections are in progress, but primarily affect the closest approach data of Voyager 1 encounter. For the preponderance of the data this effect is not important.

V.   STATISTICAL DENSITY COMPARISONS

The determination of the electron density from a propagation cutoff is

a standard laboratory procedure [Heald and Wharton (1965)]. Gurnett et al. (1981) discuss the use of a related technique (with internally generated electromatic noise, "the continuum", unable to leak out of the plasma cavity) in conjunction with the PWS broadband data obtained for a limited number of intervals of the Voyager 2 flyby. During each 48s frame of broadband data these authors have defined the minimum and maximum electron densities as evidenced by the continuum cutoff, with high precision. They have attributed the often substantial variations within these frames to apparent ($\partial/\partial t$ or d/dt) time variations; a number of these frames are at or near large, gross changes in plasma regimes as determined from the plasma time series. We have plotted the available PWS data along the horizontal axis of Figure 2 with a diamond symbol at the mean of the limits stated with horizontal error bars to indicate the range of temporal variability implied by this data. The vertical coordinate of all points plotted in this figure is the PLS electron density. When the PWS broadband intervals occurred within a calibration cycle or data gap of the PLS instrument, data for the electron density on either side of the PWS time were averaged to determine the vertical coordinate of the point; the vertical flag reflects the PLS variability during which the PWS sample was obtained. As a group the diamond points cluster near the slope one line indicating good agreement. The most discrepant of the points are associated with the calibration intervals; these comparisons are the least nearly time coincident, but are nevertheless consistent with this trend. It is fortunate for our validation arguments that these comparisons are nearly absolute and at very low densities that are indicative of the mid-latitude outer magnetosphere. They clearly indicate the capability of our analysis system to reject photocurrents which, if retained, would have caused the

apparent density in the outer magnetosphere to be nearly 4/cc as was inferred by Intriligator and Wolfe (1974) and challenged by Grard et al. (1977). This absolute comparison clearly indicates (as limited as the sample is) that the PLS electron observations below 6 keV contain the preponderance of the neutralizing electrons, even in the hotter portions of the outer magnetosphere (cf. Figure 4).

The crosses plotted in this figure are located at the abscissa determined by the PLS total ionic charge density, $n_+ = \Sigma\, Z_i n_i$, with the corresponding ordinate determined from the electron charge (equals number) density, n_- that was determined from the PLS electron data no more than 30s removed in time. It must be reemphasized that the ordinate and abscissa for this figure are in all cases from independent measurements and and analysis groups. This is especially important for the intra PLS comparisons implied with the cross data points. The use of the electron return current relation maintains the complete independence of the electron analysis. This curve represents the first actual comparison of the ion and electron charge density during the encounter over such a large dynamic range. The manner in which n_+ is determined, is discussed in detail by McNutt et al. (1981); the principle assumptions are that the macroscopic flow velocity of the ions is trans- or supersonic and that all of the ion current is found within the energy range of the PLS instrument. Under these assumptions

$$n_+ = \frac{\Sigma\, I}{|e|\, V_n\, A_{eff}}$$

where V_n is the component of macroscopic bulk flow along the Faraday cup normal, ΣI is the total measured ion current, e is the fundamental charge, and A_{eff} is the effective collector area of the cup. For the ion data the

fit determined corotational velocity along the cup normal reported by
McNutt et al., 1979 has been used, which does show departures from
corotation beyond 17 R_J, (also see Belcher et al., 1980). If a similar
determination for n_+ is made using the strict corotation at the distance
the observations were made, the n_+ data would begin to drift systematically
to the left of the slope one line. The data 1) are clearly consistent with
gross charge neutrality, 2) support the departures from corotation inside
30 R_J inferred from fitting the ion peaks when available; 3) are consistent
with the ion current measured by PLS containing more than 80% of the local
charge density as evidenced by $n_- \gtrsim n_+$ and 4) with a clear rejection of
photocurrents contribution to the electron analysis (since (a) there are no
photocurrent contributions to the ion measurements), and (b) the comparison
with the continuum cutoff measurements of Gurnett et al. (1981) is nearly
an absolute measure.

The random scatter about a slope one line slightly displaced above the
slope 1 line $n_- = n_+$ probably reflects the high level of temporal
fluctuations in the medium implicit in the PWS broadband data, and also
explicitly shown in the PLS data (f. Figure 5) since the n_+ and n_-
quantities are determined from currents that are measured serially, with
the time interval between them being ∿ 30s, and a time interval of 50 sec
to complete the entire low and high energy range of the electrons (only 4
sec for each energy range snapshot). We interpret the slight offset of
this line as an indication of the size (∿ 10%) of the unaccounted ion
charge density above the 5.95 keV PLS positive ion high energy threshold.
In addition some of the scatter may arise from breakdowns of the isotropy
assumption implicit in the approximation given in equation 1. At the
present time it is difficult to tell how important this problem is--since

our derived quantities are within the PWS variability whenever we have a measurement time coincident with the broadband coverage as can be seen in subsequent discussion. Additional mitigating factors which make it difficult to quantify this effect is that when in the magnetosphere the Faraday cup samples a conical field of view of the unit sphere with full width field of $90°$ approximately centered on the $90°$ pitch angle particles. Thus 70% of the range of pitch angles of a gyrotropic distribution are sampled in the field of view; these particles generally contribute nearly 70% of the density if the distribution is quasi-isotropic. In order for the fluctuations to be due to anisotropy effects the unmeasured 30% of the particles have to have a substantial distortion by number $7/3*(n_{true} - n_{current})$, where n_{true} is the actual density and $n_{current}$ is the one determined by the above outline procedure. Note that the present comparison includes data between 30-43 R_J, where Krimigis et al. (1979b) have suggested that a dominant fraction of the local ion plasma charge density is above 30 keV. These estimates, being parametric in the assumed composition are clearly at variance with the calibrated PLS electron charge density PLS-ion charge density comparisons. It seems likely that a different compositional assumption could reconcile the overall charge budget in those regimes. In particular if the ion population sampled by Krimigis et al., 1979b were a suprathermal proton population the inferred LECP ion density would be decreased by a factor of 4 below the oxygen assumption.

There are, in addition, several systematic anomalies within this comparison which deserve brief attention. For densities below 3×10^{-2}/cc the PLS n_+ determinations tend to scatter preferentially below the slope one line. This can be attributed to the minimum ion density ($\sim 10^{-2}$/cc)

that can be determined in this hot portion of the outer magnetosphere where the plasma is trans to subsonic (J. W. Belcher, private communication (1980)). (By contrast this density is easily measurable in the presence of the supersonic solar wind plasma). For a brief interval near an electron density of 10/cc, the inferred n_+ is below that expected on the basis of the electrons; in this interval of the hot, heavy ion plasma torus there may be some missing positive current to the PLS sensors; in addition the corotational velocity is oblique to the side sensor and there are some unresolved issues concerning the response function in this configuration in transonic flow (Belcher, and Olbert, private communications, 1980). As the density increases above this point we are following the trajectory inward to plasma regimes where the corotational flow is more supersonic where these concerns are not as severe, the spacecraft does not sample the same density regime as long and therefore noise is not so prevalent and the n_- and n_+ agreement is excellent and the scatter reduced. The measured ion density continues to climb toward a maximum charge density in excess of 1000/cc at closest approach [Bridge et al. (1979a)] and the interpretation of the PRA data by Warwick et al. (1979); Birmingham et al. (1981), appears to require an electron (not a heavy anion) density of this order of magnitude. (See comparison in Bagenal et al. (1980)). We now know that the spacecraft became negatively charged with respect to the plasma in this regime. From the excellent Voyager 1 agreement between n_- and n_+ determined before DOY 64, hour 06 we can determine the saturation curve of the return current relation (the plateau region of Figure 1) by enforcing charge neutrality, for the inner passage through the cool dense torus. When this has been done a quantitative assessment can be made of the electron density distribution and partition with energy within the cool

torus.

VI. JOVIAN PLASMA ELECTRON REGIMES

1. Solar Wind at 5 AU and Bow Shock

An example of the Voyager inbound crossings of Jupiter's bow shock and magnetopause on March 1, 1979 (DOY 60) is illustrated in Figure 3 where electron moment parameters are displayed. The upper trace illustrates the variation of the moment electron temperature; in the lower trace the electron density is indicated as directly determined every 96 seconds from the PLS electron fluxes. The self-consistently determined spacecraft-plasma floating potential is shown in the lower panel. The shock crossing between 12:26:07 and 12:27:43 SCET, occurred near local noon and was very nearly a perpendicular shock ($\theta = 91°$). At Jupiter, as at the earth, the electron plasma quantities in this circumstance indicate characteristic, abrupt, near maximal density jump (~ 4) and overshoot which is consistent with the magnetometer measurements. The electron temperature jump (~ 10) is rather large compared to that seen at earth; however, there is no theoretical limit on the size of this jump (Jeffery and Taniutti, 1964) so long as conservation of energy is not violated. The energy stored in the electron pressure change is a small fraction of the solar wind ram energy density that is lost in traversal of the shock. The directly observed unshocked solar wind before the bow shock crossing was characterized by the following average parameters: bulk velocity 400 km/s, electron density 0.5, $T_e/T_p = 2.5$ (with some variability), and plasma beta $\beta = 2$, (but ranging from 0.5 to greater than 10 in the vicinity of a large magnetic hole near 0900 SCET). The electron specific properties for this 12 hour period at 5.26 AU are that the thermal or core temperature T_c is approximately 3 eV while that for the suprathermal electrons is $T_c \sim 43$ eV.

In this interval the electron suprathermals comprise approximately 40% of the electron pressure, but only 4% of the number density. The upstream regime contains many magnetic directional discontinuities and variations in magnetic field intensity [cf. Lepping et al. (1981)]. These structures appear to be in pressure equilibrium when the actual measured electron, proton, alpha, and magnetic pressures are included. The pressure balance is achieved with a precision of better than ±10% even though there are variations in the magnetic pressure greater than ±100% during the interval. The electron pressure is usually the dominant gas pressure and the frequent anti-correlations between T_e and n_e seen in the solar wind reflects this tendency, since the plasma β for this period is usually greater than unity.

2. Magnetosheath-Boundary Layer

The magnetosheath spectra are similar in many ways to those in the earth's magnetosheath, (Montgomery et al., 1970), with characteristic flat topped distribution functions. The typical electron mean energy in the sheath is 40-60 eV. The spacecraft floating potential is reduced as expected from Figure 1 since across the shock boundary there is an increased plasma return current presented to the spacecraft while the sunlight intensity remains unchanged. Near 1715 SCET in the sheath, the electron density and temperature change in magnitude towards values that are later achieved in a full boundary layer crossing which occurs between 1930 and 2015. This is supported by the southward turning of the magnetic field direction [(cf. Lepping et al. (1981)] during this initial skimming of the boundary layer. The depletion of the electron density and enhanced temperature near the magnetopause is similar to that seen at the earth's magnetopause as has been illustrated with the ISEE data by Ogilvie and Scudder (1979), and discussed theoretically by Zwan and Wolf (1976).

After entering the magnetosphere around 20 hrs SCET the plasma becomes highly rarefied and hot with densities as low as 2×10^{-3}/cc and temperatures as high as 2 keV. The large variability shown in the magnetosphere with enhanced density and depressed temperature spikes are indications that the spacecraft skirted in and out of the boundary layer. For purposes of corroboration we point out that the density profile between 2000 and 2200 SCET matches very well with that reported by Scarf et al. (1979) using the 16 channel spectrum analyzer measurements and the assignment of the continuum cutoff to estimate the electron density.

Three traces of the Voyager electron velocity distribution function on either side of and within the durable boundary layer crossing into the magnetosphere are shown in Figure 4. The horizontal axis is the velocity the observed electrons would have had prior to being accelerated towards the charged spacecraft. In this sense the horizontal axis is the electron's speed outside the spacecraft sheath and is therefore characteristic of the ambient plasma. The vertical axis is the logarithm of the calibrated phase density in the six-dimensional phase space. The corresponding energies in decades (with respect to the plasma potential) are indicated across the top of the figure. Only points that represent measured currents above three times the noise of the instrument have been plotted in this figure. The instrument's noise level has been indicated by dashed curve near bottom of figure.

The spectrum with the triangle points is taken just on the magnetosheath side of the boundary layer, and is typical of the sheath for some distance away from the boundary layer. This spectrum has a well developed non-thermal tail as well as a prominent cooler component which comprises the bulk of the density; the characteristic energy of these

cooler particles is 26 eV. The spectrum plotted with the squares is within the the precipitous decrease of the density and temperature increase indicated in Figure 3. The principle reason for this abrupt change in macroscopic parameters is the loss of low energy plasma that is being excluded, or more correctly, extruded in the sense of Zwan and Wolf (1976) from penetrating into the magnetopause.

The suprathermal high energy tail within the boundary layer, with a characteristic energy of keV's, is seen to be enhanced by number, but with the same spectral shape as seen in the magnetosheath, perhaps indicative of magnetosphere magnetosheath interchange of electrons as the source of the non-thermal tails found in these regions. The variability in the low energy fluxes (below 140 eV) within the boundary layer is comparable to the noise level of the instrument.

3. Magnetospheric Side of Boundary Layer

On complete entry into the magnetosphere as shown by the open circle spectrum there are very few points below 140 eV that have signals greater than three times the noise. The channels in this energy range are much narrower than those above this energy and consequently they have larger threshold (dashed curve) phase densities than the higher energy channels which are considerably wider above 140 eV. This spectrum has very nearly the same spectral form of the suprathermal tail seen in the magnetosheath and the boundary layer, but with all cool plasma excluded.

On this compressed scale, the magnetospheric spectrum looks nearly flat but really spans almost an order of magnitude in phase density, so that an estimate can be made of the trend in the phase density at high energy to assess the number of uncounted electrons. By inspection it is clear that the characteristic rms thermal speed will be associated with an energy of

several keV as is shown in the moments plot where the full numerical integrations for the moment density and temperature have been performed. The outer mid-latitude magnetosphere of Jupiter appears to be filled with a sparse, hot (2-3 keV) characteristic energy electron population.

The exclusion of the cold sheath plasma from the outer portion of the magnetosphere, determines that the characteristic energy increases to an energy of several kilovolts and the densities drop precipitously to densities below 10^{-2}/cc. Nevertheless the spacecraft floating potential does not change drastically, rising to approximately 5 volts. The plasma return current to the spacecraft only drops by one order of magnitude, even though the density drops more than two and one half orders of magnitude across the boundary. Referring to Figure 1 we see that an increase in the spacecraft potential is required to retain the appropriate number of photoelectrons at the spacecraft. For reference it should be recalled that the early concerns that the Jupiter encountering spacecraft would become highly charged within Jupiter's outer magnetosphere were predicated on the "slingshot" models of Brice and co-workers of the ionospheric supply of plasma to the outer magnetosphere [Ioannidis and Brice (1971)]. This plasma was suggested to have a characteristic energy of 10-15 eV near the exobase and cooler beyond. If the outer magnetosphere had a temperature of 1 eV in conjunction with a density of 10^{-2}/cc it is clear that the spacecraft would have become charged positively in excess of 200 volts, thereby severely affecting the measurements of low energy ions as well as electrons as suggested by Mendis and Axford (1974) and others. We will show in subsequent discussion that the quantitative determination of the electron density in the outer magnetosphere is in detailed excellent agreement with continuum cutoff measurements. There can be little doubt

therefore that these densities within the magnetopause are accurate and that the return current is correctly assessed and that the spacecraft is not radically charged compared to the electron temperature which is on the order of 2-3 keV.

It follows from this discussion that the outer magnetospheric electrons are a very hot, sparse gas which differs from the interpretation of the Pioneer measurements by Intriligator and Wolfe (1974). Our finding is certainly consistent with the criticism made by Grard et al., 1977 of the Pioneer interpretation.

Taking the measured electron pressure P_e within the magnetosphere it is instructive to determine the equivalent ion pressure required in conjunction with the magnetic field to balance the solar wind ram pressure under the assumption that the magnetopause as traversed was nearly in equilibrium. The particular magnetopause crossing used for this purpose is the one which occurred toward the end of July 5, 1979, (DOY 186) from Voyager 2 inbound data. This was done because the variability in the ram pressure monitored by the Voyager 1 measurements throughout this period was not too high (refer to Figure 2 in Bridge et al., 1979b). Using a field strength of 5 gamma for the magnetic field (cf. Figure 2 in Ness et al., 1979b), ram pressure of 5×10^{-10} dyne/cm^2, and electron density $\sim 10^{-2}$/cc typical for this time period (but not shown) we get an equivalent ion temperature $T_i \sim 25$ keV which supports the suggestion by Krimigis et al., 1979a, that the outer magnetosphere contains a very "hot" ionic plasma that plays an important role in the pressure equilibrium there.

This preceding calculation only infers the dominant equivalent temperature of the ion species that dominates the ion partial pressures; it does not suggest in what energy range the preponderance of the ion

density is to be found except that it is below 25 keV. In this connection it is important to keep the comments of Belcher et al. (1980) in mind, since the energy interval of a sub-transonic plasma that contains the dominant fraction of the energy density (pressure) (e.g., Krimigis E > 30 keV), need not contain the dominant number density—especially in the case where the LECP measurements used to estimate the pressure have a finite low energy cutoff. Thus, our support for the Krimigis et al., 1979a,b estimate of the energy density is still consistent with the PLS positive ion densities (E < 6 keV) (Bridge et al., 1979a,b) being dominant in the outer magnetophere.

4. The Outer Magnetosphere

In the previous section the general morphology of the plasma electrons just inside of Jupiter's magnetopause was examined. In this section we will illustrate that portion of the outer magnetosphere where the solar wind still has an influence, but where the plasma sheet timing becomes more predictable, indicative of the growing planetary influence on this regime. For this purpose we have chosen to present in Figure 5 Voyager 2 inbound electron parameters for data acquired on July 7, 1979 (DOY 188). These data span the radial interval between 46.5 and 33.1 R_J and are presented in nearly the same format as that for Figure 3, with the exception that the position of the acquired data is explicitly indicated by an "x" and the trend of the data suggested by connecting these symbols. Superimposed on the continuous PLS density trace we have indicated the position and reported variability of the electron density determined from the broadband continuum cutoff studies of the PWS team [Gurnett et al. (1981)]. The capital "I" symbol has been used for these data, with the variability discerned within the 48s frame indicated by the extremities of the

character. The lower four panels display the magnetic field magnitude, its directions in the canonical Voyager RTN coordinate system, and the pythagorean variance as determined from 48s averages. These data have been kindly supplied by the magnetometer team to provide a framework for the discussion and interpretation of the electron plasma measurements. We have also plotted the tilted dipole magnetic latitude of the spacecraft for added reference in the panel between the logarithmic panels and the spacecraft potential.

This figure illustrates 1) the complex and apparently time variable character of the outer magnetosphere; 2) that the plasma electron definition of this regime is fully consistent with the available broadband PWS (density) and MAG (plasma, current sheet definition) data; 3) that the electrons in the plasma sheets are much cooler and denser than the surrounding mid-latitude magnetospheric plasma sampled and becomes increasingly cooler with decreasing radius; and 4) that the electron temperature on average is lower on the centrifugal side of the minimum magnetic field strength seen in each sheet crossing. Each of these points will now be developed in turn.

Complex and Variable

The spiky enhancements in the electron density and the correlated decreases in the electron temperature between 0200 and 0500 indicate the sudden, quasi-periodic appearance of electron plasma that is much cooler and denser than the hotter (2-3 keV) plasma more typical of the magneto-sphere off of the plasma sheet at this radial distance. Such spikes would ordinarily be challenged as unphysical or processing artifacts. At the low densities of these measurements incomplete rejection of photoelectron fluxes from analysis could lead to such "feed through" effects. This is

not correct and the order of magnitude changes in the density within the "spikes" are properties of the plasma indigenous to the region. This can be shown from the enhancements in the energy spectra of the electrons, but more simply, by referring to the magnetometer data plotted in this figure which show that the density enhancements are well coorelated with depressions in the magnetic intensity. Although the sampled electron pressure does rise within these spikes, its variation is insufficient by itself to be the dominant compensating energy density within the plasma sheet "spikes" traversed. Alternatively, these may not be static structures at all.

As can be seen from the temperature trace, these density enhancements are coincident with a marked reduction in the electron temperature. It should also be noted that the trend, correlation and magnitude of the density and temperature within the "spikes" are similar to those obtained when the spacecraft is located within the plasma sheet for a considerable, contiguous period (after 0445, for example) suggesting that the brief, nearly periodic (T $\sim$ 30m) density-temperature spikes may result from transient phenomena associated with the proximity of the plasma sheet—such as surface waves or time dependent equilibration of dense material that has just arrived in this vicinity via some form of flux tube interchange or other transport. Regarding the latter suggestion, cold plasma recently deposited within a flux tube may be oscillating in magnetic latitude along B, where the oscillations have not had time to damp out. This suggestion is similar to that made by Cummings et al. (1980) regarding Io's torus, and the steady state discussions made by Hill et al. (1974) interpreting Pioneer 10 measurements and Goertz's (1976b) interpretations of Pioneer 10 and 11 measurements. We conclude, therefore, that these features of high

contrast in the density and temperature profiles reflect real departures from a smooth pattern of plasma and field configurations in a steady equilibrium.

The magnitude of the density variability has been emphasized by the PWS team [(Gurnett et al. (1981)], in their study of the continuum cutoff within the sparse 48s frames of data that they have available for study. The changes within each 48s frame have been indicated by the extremes of the I character on the logarithmic plot, even though their suggested precision is three significant digits (F. Scarf, private communication, 1980). Comparisons of these data points indicate the excellent agreement between the PLS and PWS density determinations, but also indicate that the PWS variability within 48s is the "tip of the iceberg" when the continuous PLS time series is considered. The routine PLS determinations of the electron moment parameters dramatically reveal the perils of interpolation between the very accurate, but unfortunately sparse, broadband PWS density determinations. The structures between 0200 and 0500 are real, order of magnitude variations in the local density which interpolation of the broadband determinations would completely miss; a similar situation obtains between 1200 and 1400 and 1100-1200. Several of the PWS broadband determinations (e.g., 01:36, 14:11, 16:38) occur on the edge of precipitous drops in the macroscopic plasma parameters, further indicating the perils of interpolating these measurements to compare with data acquired over an interval long compared to the 96s required to determine successive plasma measurements.

The comparisons with the broadband determinations of the electron density in this very low density regime clearly establishes that photocurrents and secondaries have not been evaluated as if they were

electrons indigenous to the magnetosphere. Were this not the case the number density would be nearly 4/cc and the inferred electron temperature in the eV range (Grard et al. (1977)) rather than the 10^{-2}/cc substantiated by PWS and the keV range as reported here. The analysis procedures in this regime were not specialized to attain the level of agreement shown here, but follow the methodology outline in sections III and IV and are identical to those used everywhere within Jupiter's bow shock.

It has been previously suggested (Carbary et al. (1976)) that the time variations observed in the high energy particle data during the Pioneer inbound approaches could be due to the refilling of plasma tubes which had just been emptied into the magnetotail on the preceding planetary revolution. Until the precise origin and mechanisms of this replenishment and its equilibration can be suggested we cannot rule out this as a possible source of cold plasma and the resulting transient phenomena seen in these spikes. Alternatively, the extant discussions of flux tube interchange motions (Gold (1959), Sonnerup and Laird (1963), Hill (1976) and Chen (1977)) suggest that the temperature of the plasma in the final state is usually no greater than that it had been before the flux tube became interchange unstable. In this connection it is important to note that the temperature (mean energy) of the electrons in these spikes is considerably larger than the electron temperature found in the very dense portions of the Io plasma torus, but becomes comparable to the electron temperatures on the outermost portions of the plasma torus proper; thus, interchange motions most recently with the outer portions of the plasma torus ($\sim 9 R_J$) is another possible candidate to explain the spike morphology in the outer magnetosphere.

Plasma Sheet Correlation with $\underline{B}$ (t)

The durable and transient density enhancements of the plasma sheet are observed to be in close association with the diamagnetic depressions and directional changes defined by the magnetometer data. In general the data are consistent with cooler electron plasma being confined in a plasma sheet (approximately $\pm 7°$ magnetic latitude in width) which extends (near noon local time) beyond 40 R_J. Because of its confinement to small magnetic latitudes, the origin of this cooler plasma is probably ultimately one of the Galilean satellites (Hill and Michel (1976), Siscoe (1977)), with Io the most likely source as indicated by the observed active volcanism [Morabito et al. (1979)] and plasma torus discussed in the introduction. The plasma within the sheet has temperatures and densities that are markedly different from the mid-latitude regions which bound the sheet. In this mid-latitude region, at this radial position the typical densities are 10^{-2} and the characteristic mean energy of the electrons is in the vicinity of several keV. As noted previously for the transient sheet, the temperature, T_{sheet}, in the durable plasma sheet, though cooler than its mid-latitude surroundings, is still much higher than that characteristic of the dense portions of the Io torus; in addition T_{sheet} is an increasing function of jovicentric radius; these facts argue for a complicated and probably energy dependent egress of the electrons from their "source" to their current location within the sheet.

Although there is good correlation between the field and plasma signatures at the sheet at 0730, 1230, 1600, 1900, 2230 SCET, there is no single ten hour wave that describes the arrival of the sheet. Before the clear 180° lambda angle crossing of the magnetic current sheet near 1230, the plasma and field show a compatible but irregular pattern. As indicated in the dipole magnetic latitude, λ_m, trace on this figure, the expected

current sheet crossing at 0200 did not occur, and the observed field indicates the spacecraft is north of the actual magnetic equator while it should have been south of an undistorted plasma sheet if it were coincident at this distance with the dipole magnetic equator. The incomplete current sheet traversal at 0430 did occur "on-time" for a S-N crossing. We therefore suggest that the spacecraft during this period ($\sim$ 40 R_J) was slightly above the plasma sheet that has been bent down from the dipole equator indicating the external influence of the magnetopause currents driven by the solar wind. The sheet traversals after 1200 are "on-time" with respect to the trajectory and the dipole equator, except for the "spurious" incomplete plasma sheet penetration centered at 1900 SCET. Between the plasma sheet encounters at 1600 and 1900, at approximately 1745 SCET there was an abrupt increase in the magnitude of B with no angular change, which may have been the signal of the change in the external conditions of the solar wind ram pressure reported by Bridge et al. (1979b), Figure 3. It is therefore possible that the "spurious" sheet encounter at 1900 resulted from this change in the external conditions with the plasma sheet having been pushed up toward the spacecraft. By the Pioneer conventions this regime is clearly within that called the outer magnetosphere.

The plasma sheet crossing at 1230 is another example where external conditions may have had an influence. Near 1200 SCET the spacecraft begins to enter the plasma sheet, crossing the current sheet or magnetic equator at 1230. After this time, it suddenly leaves the plasma sheet before reentering at about 1250 before finally emerging around 1310. Here it appears the plasma sheet moved suddenly above the spacecraft possibly by some change in the external conditions before returning to its equilibrium

position. However, for this event, no significant change in the external conditions are predicted by the Voyager 1 data in Bridge et al. (1979b). Therefore, some alternative explanation maybe required, or the Voyager 1 spacecraft did not observe the change in solar wind conditions experienced by Jupiter's magnetosphere at this time.

Electron Temperature within and Along the Plasma Sheet

The electron temperature variations during this day within the plasma sheet reveal an interesting pattern: being generally cooler on the side of the sheet more nearly connected to southerly magnetic latitudes ($\lambda \sim 0$; 360° (for inbound data)) than northerly ones ($\lambda \sim 180°$). Examples of this effect can be seen at 0500 (N-S), 0600 (S-N), 1600 (S-N) and 300 (N-S), where the expression in parentheses indicates the direction of the magnetic hemisphere traversals along the trajectory. Even the current sheet crossing at 1230 shows this effect, with the transient effect just discussed complicating the picture. More generally there are many "spiky" signatures throughout the plasma sheet crossings which are randomly distributed in magnetic latitude, that have been visually smoothed over in suggesting this pattern. As previously noted and discussed in detail in the next section, we believe these transient spikes are the result of newly added cold plasma to these parts of the plasma sheet which may be bouncing in magnetic latitude along B and have not yet come to equilibrium with the plasma sheet populations. Geometrically, the nearly fixed jovigraphic latitude of the spacecraft on this day determines that the centrifugal "equator" will be encountered on the southerly extremities of the plasma sheet, i.e., on that side of the magnetic equator where the field line vectors are pointing toward the planet. By the usual steady state arguments (cf. Hill et al., 1974 Goetz (1976a) and Cummings et al. (1980)

and reference, therein) cooler plasma within the sheet should be found towards the centrifugal side of the magnetic equator and the hotter plasma would be preferentially observed towards the magnetic equator. In some average sense this is the pattern we have observed. We will also illustrate this effect in the middle magnetosphere section for inbound and outbound plasma sheet crossings.

The electron plasma distribution functions sampled within the plasma sheet reveal a non-Maxwellian distribution of speeds and suggest that the probability distribution function pattern observed results from the kinematic intermixing of two different space-time history populations in much the same way as recently discussed for the solar wind distribution (Scudder and Olbert, 1979a,b), with the suprathermal population coming most recently from the hot mid-latitude plasma reservoir and the thermal portion perhaps arriving at the point of observation by "interchange" motions. Although not illustrated the mean energy of the thermal subpopulation of this non-Maxwellian distribution within the plasma sheet in the outer magnetosphere ranges between 50 and 300 eV, with the more typical value of 100 eV (which is compatible with the hot outer Io torus discussed later). As we have seen the plasma sheet is juxtaposed to a hot, sparse reservoir of 2-3 keV plasma which seems to be present at all mid-magnetic latitudes sampled. This hot population can symmetrically penetrate the plasma sheet population from both hemispheres, with very little Coulomb impediment, especially since the plasma sheet is so sparse in an absolute sense.

The partition of number density between the thermal and suprathermal electrons within the plasma sheet is nearly even with $n_c \sim n_h$ at 40 R_J. As the radial distance gets smaller we have noted that the cooler thermal subpopulation fraction of the density is increasing. We will illustrate

this trend with data in the next sections of the middle magnetosphere and within Io's plasma torus. These facts are consistent with the source of the cooler, thermal subpopulation being inside of the observers radial location; this source of plasma is increasingly diluted by filling a larger volume as it moves radially out from its source.

The observer within the plasma sheet samples (at any given time) an electron population that is a mixture of these two types of plasma populations. At varying radial positions along the sheet, the relative mixture between these hot and cold populations determines the actual mean or thermal energy reported by an observer, viz,

$$T = (n_c T_c + n_h T_h)/(n_c + n_h),$$

where n_c and n_h, and T_c and T_h are the densities and mean energies of the thermal and suprathermal populations, respectively. Depending on which source is the dominant supplier of partial pressure to the observer, either limit of the temperatures of the respective sources can be attained: near the boundary layer at the magnetopause it would appear that the "cold" source has been effectively diluted and $T \sim T_h$; as we approach the planet T is observed to decrease indicating that the cold source is increasingly providing the dominant partial pressure to the vicinity of the observer. This pattern is consistent with Io as the cold plasma source, and the hot bath reservoirs at the mid-latitude regions being the source of hot plasma. Mid-Latitude Region: Exospheric or Acceleration?

It is not clear that the higher mean energy outside of the plasma sheet necessarily requires any acceleration per se of the electrons, since this high mean energy is realized at a very low density, with the energy density of the electrons not possessing a strong variation over the latitudes sampled, even though the density and temperature do. It is possible that

this distribution is a natural result of the "zenopotential", which is the renamed version of the geopotential of Angerami and Thomas (1964), which has been studied by many authors in connection with the behavior of ions at Jupiter (cf. Goertz (1976a) and references therein). At the ionosphere gravity acts to stratify the plasma, with the peculiar, higher energy electrons escaping its pull; at the centrifugal "equator" a similar stratification is produced with the effective gravity implied in the centrifugal force, again leaving the higher energy ones free to escape. Thus each field line that threads the plasma sheet is connected to two different exobases, with the mid-latitude regions being "above" both of them. It would seem quite natural that in steady state those electrons which can be found in this intermediate region should have an energy higher than either of the base temperatures and at a much lower density than at either exobase. This is certainly the case in this situation; however whether such a segregation of keV electrons to mid-latitudes is actually realized or whether acceleration is actually required must await a detailed evaluation of this idea.

Summary

This sample of the outer magnetosphere data has illustrated six main points: 1) the ambient electron plasma within Jupiter's magnetosphere does participate in the formation of the diamagnetic plasma sheet as defined by the in situ magnetometer data; the density enhancement in the sheet primarily results from an increased fraction by number of cooler electrons; 2) the electrons are cooler on the centrifugal side of the sheet than on the magnetic equator side; 3) the typical electron densities in the mid-latitude outer magnetopheric regions sampled are in the vicinity of 10^{-2}/cc, with the electron temperatures in this regime on the order of

2-3 keV; 4) the enhanced density within the plasma sheet is non-Maxwellian
distributed and accompanied by a reduced average random energy
(300-800 eV); this minimum temperature within the sheet appears to be an
increasing function of the radial distance; this thermal density is also an
increasing fraction of the total density in the sheet as the planet is
approached; 5) there is much variability in the time series on the time
scale of 96s surveyed in the outer magnetosphere--this time dependence is
most prominent within and very near to the plasma sheet proper; and 6)
quantitative agreement is excellent with the very accurate, but sparse, PWS
broadband determinations of the electron density.

5.   The Middle Magnetosphere

In this section we focus our presentation on two examples of plasma
sheet crossings within the middle magnetosphere. These examples have been
chosen to illustrate the observed electron properties within the plasma
sheet in more detail than previously shown for the outer magnetospheric
sheet. The principle features to be illustrated are that the density
temperature anti-correlation noted in the outer magnetosphere persists; 2)
the mean temperature in the sheet is further reduced as we approach the
planet; 3) the temperature distribution within the plasma sheet is
consistent on the inbound and outbound current sheet traversals with the
pattern seen in the outer magnetosphere--being cooler on the centrifugal
side of the magnetic minimum; and 4) to illustrate that the electron speed
distribution within the sheet is markedly non-Maxwellian with the largest
cold to hot density ratios occurring within the plasma sheet and the
suprathermal density is symmetrically enhanced about the magnetic equator
proper.

Plasma Sheet Morphology

Data from the inbound traversal of the Voyager 1 spacecraft of the plasma sheet at 16.9 R_J are illustrated in Figure 6. These observations were acquired on March 4, 1979 (DOY 63). In the upper panel the variation of the total electron density, n_e, and the suprathermal portion of this density, n_h, are shown. The hot density, n_h, is determined by direct integration over the suprathermal phase density defined by

$$f_{hot}(v) = f(v) - f_{cold}(v),$$

where f_{cold} is the best fit Gaussian to the thermal population and the integral is of the form in equation 1. Care has been exercised to limit the range of integration to only those energies above which the Gaussian representation $f_{cold}(v)$ is less than 50% of the observed phase density $f(v)$. (The thermal population are well fit by Gaussians as discussed below in connection with Figure 7). The second panel illustrates the variation of three separate statistics of the electron distribution, which characterize the spreads of the distribution: 1) the total moment defined temperature, T_e, as per equation 2; 2) the thermal spread, T_c, of the low energy population determined by a Gaussian fit; and 3) the effective mean energy of the suprathermal population, T_h, as determined from the other parameters via partial pressures. The remaining four panels illustrate the magnetometer data in the same format as that for Figure 5, being 48s averages and kindly provided by the MAG team to facilitiate our discussion of this data.

The plasma sheet defined by the electrons is a region of enhanced density above the general background increase of the density profile; the sheet proper is not always a monotonic enhancement over the ambient profile, since it is punctuated at times with many temporal (or convective) perturbations. The total density enhancement over the ambient in this

example is nearly a factor of 4-5, while the suprathermal density is only enhanced by ~ 50%. The hot (suprathermal) density enhancement is very nearly symmetric with respect to the magnetometer lambda angle, suggesting that it is concentrated in absolute terms and symmetrically distributed about the magnetic equator as expected in theory (Hill et al. (1974), Goertz (1976b), and Cummings et al. (1980)). (In this connection it should be pointed out that the magnetic depression in the rapidly increasing main Jovian magnetic field is slight; the magnetic lambda angle change in this circumstance is a convenient marker for the magnetic equator.)

The enhancement in the total density is accompanied by the now familiar reduction of the mean electron temperature. At the minimum of the magnetic intensity within the sheet the observed temperature was as low as 100 eV as contrasted with the external values of 300-400 eV seen before 1800 SCET. This value is lower at this radial distance than comparable values seen in the outer magnetosphere (cf. Figure 5). This temperature is on average lower on the centrifugal side ($\lambda = 0°$, $360°$) within the sheet than on the magnetic equator side and is precisely the pattern observed in the outer magnetosphere and illustrated in Figure 5. The thermal subcomponent temperature appears coolest ($T_c = 10$ eV) in a one sided manner near the observed magnetic minimum, being depressed by nearly an order of magnitude with respect to the thermal mean energy seen outside the plasma sheet proper. The lowest observed thermal temperature in the densest portion of the sheet is compatible again with characteristic temperatures in Io's plasma torus. By contrast the mean suprathermal energy is relatively unaffected during the sheet traversal, being reduced on the order of 20% with respect to external conditions.

The traces of these derived quantities lend credence to the suggestion

that the suprathermal populations observed within the plasma sheet are global populations that are not especially confined to the vicinity of their observation. By contrast the thermal population which contains the preponderance of the density are localized in a neutralizing response to the enhancement of the centrifugally entrained ions. This situation is similar in many ways to the solar wind, with the inhomogeneity of the system ultimately dictating the mix of local and global populations seen in any locale.

The density profile of the plasma sheet enhancement is not always monotonic, even when passed through a low pass filter, usually displaying a multi-maxima profile as in this example. The first density enhancement in the plasma sheet per se does not correspond to the abrupt magnetic signature of the "current sheet" traversal as indicated by the polar angles of the magnetic field. This latter signature does accompany the extreme density maximum just after 1900 SCET. In the first of these density peaks, McNutt, Belcher, and Bridge (private communication (1980)) report the largest average mass (amu), whereas in the second (extreme) maximum the average amu of the ions is lower and the ions below 6 keV are coolest. As noted earlier the (total) electron temperature, T_e, is a minimum (with large variability) in the vicinity of the first density maximum which we have interpreted as the centrifugal extreme of the plasma sheet; this interpretation is consistent with the slightly higher average amu suggested for the ions found there. Initially it appears difficult to reconcile the ions being coolest in the vicinity of the magnetic equator extreme of the plasma sheet. However, it should be recalled that the minimum of the electron temperature is reflected in the total or moment temperature, whereas the ion temperatures below 6 keV pertain to fits to Maxwellian

forms. Since the contribution from suprathermal ions are probably important in the pressure balance in the sheet these contributions could be substantial. The contribution to the ion pressure from fluxes above 6 keV (i.e., suprathermal tails) must be considered before there is a real conflict between the electron and ion observations and theory.

Rapid fluctuations in the densest portion of the plasma sheet are commonly observed in the middle and outer magnetosphere. This variability in the moment parameters arises primarily from the changes of the density and temperature of the thermal subpopulation of the plasma. The periods of these variations in this middle magnetosphere example is approximately 7 min, which is shorter than the characteristic 30 min period of the fluctuations noted in the outer magnetosphere in Figure 5. This Figure and Figure 8 together with Figure 5 illustrate that the position of these spikes within the plasma sheet is more or less random with respect to magnetic latitude within or very near the sheet proper. Thus the profile of the cooler thermal population is more chaotic and on any given sheet traversal is probably not in its expected equilibrium position. These circumstances may additionally alleviate any apparent disagreements between the ion temperature morphology below 6 keV, the electrons, and theory.

In Figure 7 we have exhibited the speed distributions of electrons observed at the times indicated by the arrows in the moment parameter plots of Figure 6. The motivation for a multi-component, non-Maxwellian parameterization is immediately clear, since a simple Maxwellian in this format is a parabola. To point out how far the electrons (and probably the ions) are removed from thermal equilibrium it is interesting to note that within the sheet on this day the number fraction of the suprathermal electrons is only 8%, whereas this subpopulation comprises nearly 88% of

the electron pressure! This is an example of an astrophysical plasma with its internal energy density distributed in a way that is atypical of previously sampled space plasmas. This electron distribution which has been directly sampled with one instrument (PLS) may be a prototype for understanding the seemingly contradictory ion morphology (PLS vs LECP) in the outer magnetophere discussed by Belcher et al. (1980).

There are usually many low energy channels available to define the Gaussian representation for the low energy regime. The best fit for the lower energy domain are indicated by the dashed parabolas and were used to determine n_c and T_c in the usual way; the normalized chi-square for these fits and those within the sheet is generally of order unity indicating very good fits. The fits and the data clearly show the substantial changes in the equivalent width of the thermal regimes of these spectra as the plasma sheet is traversed. By contrast the suprathermal tails above the fit regimes do not change as much during the sheet traversal--this being a dramatic example that energy dependent processes do not permit $f_{e(\underline{v})}$ to evolve in a self-similar way.

The many point definitions of a cool (approximately 10 eV) Gaussian distribution of electrons within the sheet would argue that these electrons have their origins in regimes of near collisional equilibrium, perhaps within the Io torus and observed within the plasma sheet as a result of interchange motions. These low energy electrons in the plasma sheet would ordinarily have a very long range against Coulomb collisions, were it not for the large polarization potential which they must overcome before leaving the plasma sheet. This potential is on the order of the mean electron temperature in the center of the sheet and effectively confines the predominant fraction of the electrons to bounce (electrostatically

mirror!) back and forth across the plasma sheet. This does not imply that the electron density is necessarily bunched by such a bounce motion, but rather that a given electron can kinematically execute bounded trajectories within the sheet being impeded electrostatically not to stray too far from the densest portion of the sheet. Of course the more energetic of the electrons have sufficient energy to get out of this electrostatic trap, but the thermal electrons (because they have much less than the average energy) will be ensnared by this potential well. If the residence time in the plasma sheet can be made very long by this process, it is possible that local self-Maxwellizations could be in progress in these regions. This interpretation would be consistent with, but not definitive of, a closed magnetic topology at these radial distances on both the night and day side of the magnetosphere, since the time interval required for this process is many Jupiter rotations.

The other example of detailed data of this type is illustrated in Figure 8 where derived parameters from fluxes from the identical Voyager 2 instrument on the outbound leg are presented in the same format as those in Figure 6. These data were acquired on July 7, 1979 (DOY 191) at 12.87 R_J. In this traversal the plasma sheet density enhancement is more regular, but still punctuated by significant variability (T ∿ 7 min) in the thermal component parameters. It should be noted that the fluctuations are confined near the sheet. As seen previously, the average and thermal temperature are depressed significantly relative to the surroundings; the suprathermal temperature changes very little across the sheet. The background of the profiles reflects the radially decreasing density and increasing temperature profiles that are consistent with the earlier trends discussed. As in the inbound middle magnetosphere plasma sheet crossing,

the suprathermal density enhancement is nearly symmetric with respect to
the magnetic equator as indicated by the polar angles of the magnetic
field. As in the pattern noted earlier, the total electron temperature
within the sheet is cooler on the southern magnetic latitude portion of the
sheet, which is consistent with it being the centrifugal extremity of the
sheet. (Note that the magnetometer coordinate system is a sun centered
coordinate system, so that on the outbound leg of the orbit southern
hemispheric field lines are lambda angles in the vicinity of 180°, while
northern hemisphere lines have $\lambda \sim 0°$, 360°.)

The companion spectral plots at the position of the arrows in Figure 8
are shown in Figure 9 illustrating the generality of the patterns in the
microstate established on the inbound crossing within the inner
magnetosphere. As the plasma gets denser it becomes cooler upon entry into
the sheet, leaving the suprathermal phase density essentially unmodified in
structure or spectral shape.

Plasma Sheet Gyro-harmonic Emissions

Many theories of gyro-harmonic Bernstein-like electrostatic emissions
(cf. Young et al. (1973), Ashour-Abdalla et al. (1979) and Birmingham et
al. (1981) and references therein) suggest that the presence of these
emissions can be understood if 1) the electron phase space is more
complicated than a simple Maxwellian and 2) that varying patterns in the
gyro-harmonic structure can be produced depending on the thermal to
suprathermal density and temperature ratios. As shown in Figures 4, 7, 9,
10 and as we have repeatedly argued, the observed PLS electron distribution
functions are almost always non-Maxwellian; at times the observed
distributions can have varying number fractions within the thermal and
suprathermal populations. Usually, but not always, when the number density

is enhanced, the total increase is a result of the preferential enhancement of the thermal populations. This is especially true in the plasma sheet proper as shown in Figures 7 and 9 and the spikes that have been observed in the outer magnetosphere. In this way the fraction, $n_c/(n_c + n_h)$, of electrons in the "thermal" population is enhanced in these places; according to these theories this situation increasingly favors these emission mechanisms. In this connection the PWS team has reported evidence for enhanced electrostatic emissions inside 23 R_J near the "upper hybrid frequency in the dayside outer magnetosphere... between higher harmonics of the electron gyrofrequency," (Kurth et al. (1980) and references therein). These authors discussed one of the current sheet crossings illustrated by the PLS data shown in Figures 6 and 7 and inferred that the electron distribution functions should have a two temperature structure as we have now explicitly shown in Figure 7. As also shown in Figure 6 the thermal density is upwards of 80% of the total which is in marked contrast to the sheet of the outer magnetosphere where $n_c \sim n_h$ and is perhaps the reason for localization of the banded emissions within the inner magnetosphere since n_c/n_h is increasing with decreasing distance (cf. Torus section).

6. Electron Properties in Io's Plasma Torus

Direct in situ measurements within Io's torus of electrons have been made by the PLS experiment which bear directly on the interpretation of the optical measurements as well as the definition of the plasma environment in this prototype, as it were, of a planetary nebula. We will illustrate 1) that the system is demonstrably removed from local thermal equilibrium, 2) that the electron bulk parameters possess important and sizeable macroscopic and microscopic variations with radius and magnetic latitude within the torus, and 3) that a sample of these regimes are compatible with

selectively inferred properties of the plasma torus made by essentially
indirect methods. As is already known, Io's plasma torus during the
Voyager 1 encounter was unusually dense, reaching densities beyond several
thousand per cubic centimeter. In this circumstance we now know that the
spacecraft did achieve a negative potential, which has left our reduced
data base temporarily incomplete pending further analysis, especially in
the densest portions of the torus. For the present we will illustrate the
extreme situations that are known from data with three spectral examples.
These examples were also selected with an eye toward establishing contact
with the burgeoning number of indirect inferences of the plasma torus
properties discussed in the introduction.

The spectra we will show are representative of three relatively
well-defined subregimes of the plasma torus that are delineated by abrupt
changes in the characteristic electron temperatures: a) the hot/outer
torus $\gtrsim$ 100 eV, b) the temperate/middle torus $T \sim$ 10-40 eV and the
cold/inner torus $T_e \lesssim$ 5 eV. We are not in a position to completely define
the spatial limits of these regimes, but can illustrate the electron
properties within each of them. We do not suggest that the spectra shown
are neccessarily typical of these regimes. Our principle emphasis is to
establish that the plasma torus is <u>not</u> a volume of isothermal, Maxwellian
distributed plasma--but, rather an inhomogeneous entity in density,
temperature and microstate. This experimental fact complicates the
interpretation of line of site measurements; however, in order to extract
the maximum information from such integral measurements, the community
should be aware of the observed structure in the electron macroscopic and
microscopic parameters and that the system is not in local thermal
equilibrium. However, the general magnitude of the electron temperature

especially in the outer two zones is adequate to support the collisional ionization of sulfur in places to the doubly or triply ionized states reported by Broadfoot et al. (1981).

A composite diagram composed of a sample of electron distribution functions from each of the above regimes is presented in Figure 10. From left to right the distribution functions refer to decreasing radial distance from Jupiter and also from Io. In each panel the Jupiter centered angular separation, ϕ_{Io}, between the spacecraft and Io and the dipole magnetic latitude, λ_m, are indicated. Also included on each spectrum are the derived statistics for the thermal and suprathermal populations. All of these spectra have well-developed thermal subpopulations, which like the plasma sheet enhancement spectra, can be well modeled by a Gaussian distribution. The width of the thermal component appears to be a decreasing monotonic function of the radius, but it is clear that the density is not. This is consistent with earlier definitions of the torus (Bagenal et al. (1980)) and that the trajectory progresses inside the annulus of the torus between spectras 2 and 3. To varying degrees all of these spectra show evidence for a well-developed suprathermal tail which illustrates that none of these regimes is in local thermal equilibrium wherein the electrons would be distributed according to a single Maxwellian. The torus is a regime of very strong density gradients not only within the torus, but the contrast between the peak torus density and the 10^{-3}/cc observed in the outer magnetosphere is nearly as severe as that from the edge of the corona to the 1 AU observer in the solar wind. In such radical inhomogeneities, strange non-thermal spectra are to be expected as has recently been discussed in connection with the solar wind (Scudder and Olbert, 1979a,b).

As Io is approached, the mean and the thermal population of the electrons become cooler; however, the values at 14:24:36 of 5.0 eV are not the coolest temperatures witnessed. The collisional lifetime of the neutral sodium atoms is a sensitive function of the temperature of the electrons which can collisionally ionize it. With its low ionization potential of 5.3 eV, any asymmetry in the ionizing plasma electron temperatures with respect to Io's orbit could play a role in understanding the puzzling patterns of the resonantly scattered sunlight off of the neutral sodium reported by ground-based observers and discussed in the introduction.

The middle distribution function, indicative of the temperate region, was also selected to establish contact with the indirect inference by Coroniti et al. (1980). These authors suggested at this time and location along the trajectory that suprathermal electrons (1.1% by number and characteristic energy of 1 keV) were required to explain the plasma hiss noise detected by the PWS instrument. As seen from the derived parameters within this panel, the suprathermal population, above the fitting regime of 240 eV comprise 1.4% of the ambient electron number density. Allowing that not all of the suprathermal electrons counted in this way can be resonant and that the mean energy of the suprathermal electrons is observed to be 1.2 keV (although not Maxwellian distributed!), the direct PLS electron measurements and the indirect PWS inference are in remarkable quantitative agreement.

This spectra also illustrates that the suprathermal fraction of the number n_h/n_e density is larger than seen in the inner torus but still less than the hot fraction seen in the outer torus. This pattern is consistent with the trend noted in the outer and middle magnetosphere, with the hot

number fraction growing with distance, while the overall number density is declining.

The temperature of the electrons in the middle and outer portions of the torus are clearly capable of permitting collisional ionization of sulfur and also collisionally exciting SII and providing the optical emission reported by Kupo et al., as well as a wealth of other EUV emissions that have been reported by the Voyager EUV team. It must be emphasized that the non-thermal distributions imply that estimates of cross sections based on the apparent thermal spread of the component which is dominant by number could seriously be in error. In such a non-Maxwellian plasma, the evaluation of rate processes requires a full convolution of the energy dependent cross section with the observed energy distribution of the the electrons. It is anticipated that this effort will be undertaken in a future study to contribute to the unraveling of the line of sight effects embedded in the spectroscopic measurements.

The outermost example of the torus has a mean energy of 120 eV, while the effective temperature of 92% of its distribution is 26 eV; the suprathermal electrons at this position possess four times as much partial pressure as the more copious thermal population. It would appear that various atomic processes as ordinarily parameterized could be variously more sensitive to either or both of these subpopulations: clearly collisional ionization rates will be sensitive to these suprathermal tails, whereas recombination rates are more sensitive to the effective temperature of the more numerous thermal particles. In short the "canonical" methods invoked by Brown (1976) to remotely infer the density and temperature of the electrons within the torus do not apply in this first example of a "planetary nebula" that has been sampled directly. A relaxation of the

Maxwellian distribution assumption for electrons embedded in this theory appears to be required. As argued in connection with the solar wind distribution functions (Scudder and Olbert 1979a,b), the inhomogeneity of the plasma system connected to the point of interest determines the departures from local Maxwellian behavior. Clearly, the most general aspect of a planetary nebula is its proximity to the gravitational focus of the nearby planet; therefore the radical spatial inhomogeneities witnessed in the torus at Jupiter (where centrifugal forces produce the "effective" gravity) are rather general properties of such systems and so, apparently, are the non-Maxwellian features that have been observed. To some extent the wide range of observed values of electron density and temperature present in the line of sight of the optical measurements, makes it somewhat artificial to argue that LTE was not so bad an approximation for the actual circumstance of the torus plasma. In the future these canonical methods will have to be improved, or, lacking this improvement, taken somewhat less seriously.

Menietti and Gurnett (1980) have attempted to bound the electron temperature of Io's torus from the Landau damping characteristics of whistler mode radiation on the assumption that the torus inside of L = 6 is isothermal and that the electron distribution is Maxwellian everywhere along the ray path. Their limits of 2-3 x 10^{5}° K (20-30 eV) are certainly consistent, though higher than the locally sampled 6.3/5.5 eV (T_e/T_c) temperatures that have been directly inferred in this inner regime. The bounds placed by these authors probably pertain more to the highest electron temperature in the mid-latitude torus along the ray path. This regime was probably not sampled directly, but such temperatures, as we have seen are not unusual at other magnetic latitudes as for example shown in

the middle spectra of Figure 10 or in the outer and middle magnetosphere (Figure 5, 6-9).

The PRA group (Birmingham et al. (1981)) have inferred that the electron temperature ratio T_c/T_h of the "cold" (thermal) to "hot" (suprathermal) population should decrease as the spacecraft moves from the hot outer torus towards the cool inner torus. This prediction is based on a modeled distribution function that may not fit the actual data. However, the trends they suggest in their T_c/T_h parameter is observed (cf. Figure 10a,c) although thorough quantitative tests of this prediction must be deferred until the complete torus data set is reduced.

On the whole we can say that the correspondence between the indirect inferences of the torus electron properties and the direct in situ measurements of them are in unusually good agreement, especially by the canonical standards of astrophysical arithmetic.

VII. SUMMARY

The survey just completed has defined, for the first time, the state of the electron component of the plasma within Jupiter's magnetosphere. This survey has not attempted to define nor preclude local time variations within Jupiter's magnetosphere. The quantitative corroboration for the inferences of this survey are excellent. Statistical and direct comparisons have been performed to validate the estimates of the ambient density, to assure the community that spacecraft sheath plasmas were not being considered as indigenous to the zenophysical regime being explored. Detailed comparisons with the density determined from the continuum cutoff method of the PWS experiment show excellent quantitative agreement, even when the density is as low as 5×10^{-3}/cc in the outer noon magnetosphere.

We have also illustrated the benefits of directly determining the

electron charge density. An illustration that assignments of observed plasma radiation "lines" are often subjective can be found in the articles by Gurnett et al. (1979) and Warwick et al. (1979b), where disagreement on the upper hybrid line identification yielded local density estimates at Voyager 2 closest approach with a spread of 39(PWS) - 450(PRA)/cc! The in situ PLS electron density at 2230 on July 10, 1979 is $n_- = 29.9$/cc whereas PLS ion charge density reported by McNutt et al. (1981) is 30.8/cc. This density yields an upper hybrid frequency of 49.9 khz which is well within the PWS 15% (3db) bandwidth of the 56 khz channel. These direct measurements support the interpretation of the PWS team, and provide a resolution of the uniqueness problems of some of the plasma wave indirect methods. Kaiser and Desch (1980) have recently also concluded by independent arguments that the previous PRA interpretation was in error.

The comparisons of the PLS n_- and PLS n_+ densities of Voyager 2 closest approach agree at much better than the 10% level as discussed extensively by McNutt et al. (1981). Using the constraints of the charge budget we can infer that the fluxes above 28 keV reported by Krimigis et al. (1979b), (1981) infer cannot be oxygen since this would violate local charge neutrality; a compositional assignment with substantially lower amu (such as protons!) could render a local charge budget balance. Clearly, the electron density can assist in these decisions in the future.

The emerging picture of the electron plasma in the magnetosphere is that the outer magnetosphere is a hot (2-3 keV), sparse ($10^{-3} - 10^{-2}$/cc) regime, which more or less is present at all magnetic latitudes sampled, that envelopes the plasma sheet which is formed in the presence of Jupiter's enormous centrifugal forces. The plasma sheet when observed contains electrons of lower average energy than the surroundings; however,

this regime has a complicated microstate with non-Maxwellian distribution functions. The suprathermal population of electrons within the plasma sheet appear to have most recently come from this hot enveloping reservoir of 2-3 keV electrons which presumably dominates the mid-latitude range of the magnetosphere. The thermal component of the microstate within the plasma sheet, is more variable and generally has at least half of the total ambient density. The thermal population is often distributed in energy within these sheets as if in a Gaussian way with a characteristic energy width at 40 R_J as small as 50 eV.

The plasma sheet sub-population properties have been monitored and these data suggest that the average temperature within the sheet (while always cooler than its immediate off sheet surroundings) is decreasing as we approach the planet. Microscopically, this arises because the mix of cooler thermal populations which seem to supply the thermal regime of the electrons is getting stronger than the supply of suprathermal phase density from the hot reservoir above the sheet proper. Consequently by the law of partial pressures the average temperature of the electrons in the plasma sheet decreases, until within Io's torus the average temperature of the electrons is nearly that characteristic of the thermal subpopulation. We have therefore tentatively identified the vicinity of the Io torus as the most immediate source for the cool electron thermal populations seen within the plasma sheet. We have also suggested that the time variability witnessed in the vicinity of and within the plasma sheet may be indicative of interchange motions that were actually in progress that were bringing torus material out to the distant magnetosphere, even as the observations were being made. It is by no means clear that the theories of interchange motions have seriously considered what the thermodynamic signatures of such

motions should be for the electron portion of the plasma. This is
particularly troubling since the interchange process proceeds on a very
slow (MHD) time scale, whereas the temperature signatures of the electrons
within these stratified flux tubes can change dramatically because of the
inordinate mobility of the electrons.

It has been suggested that the existence of the hot mid-latitude
reservoir in the magnetosphere may not necessarily require acceleration per
se since these regions on closed field lines are in the peculiar situation
of being simultaneously above two different exobases: one at the
ionospheric foot of the flux tube, with the other at the centrifugal
equator. In this situation a small sub-population of the electrons that
can escape the respective exobases will find a natural place in the
mid-latitude regions. The need for ancillary acceleration awaits detailed
modeling of this situation.

We have illustrated some initial phases of this thermal stratification
near the centrifugal equator, by illustrating the empirical fact that the
mean energy of the electrons is cooler on the centrifugal side of the
magnetic minimum within each plasma sheet discussed in the paper, both in
the outer and middle magnetosphere. We also have illustrated that the
suprathermal electron densities that have characteristic energies of
kiloelectron volts, are symmetrically enhanced about the magnetic equator
as predicted by the usual steady state theories.

The preferential enhancement of the cooler electron population seems to
have exceeded some important minimum value within 23 R_J, since the PWS team
reports banded gyro-harmonic emissions only inside of this distance, while
the purportedly responsible two component electron distribution functions
are observed at all radial distances that the plasma sheet has been

directly observed.

The in situ electron properties of the Io plasma torus have been initially surveyed. By direct observation the electron distribution function is not a simple Maxwellia, but posseses suprathermal populations which clearly indicates that e-e collisions have not been sufficiently frequent to define a local thermodynamic state. By inference the ions cannot be in temperature equilibrium with the electrons since the time scale for this process is longer, the ratio of scales going like the ion-electron mass ratio. The survey has been limited to date by the spacecraft becoming negatively charged, which has hampered a portion of our data reduction. We have identified several systematic variations in the microscopic and macroscopic electron parameters between 8.9 and 5.5 R_J. There appear to be at least three electron regimes with differing mean temperature; these regimes have been named the outer (or hotter), the middle (or temperate) and the inner (or cooler) torus; these three regimes have mean energies of 100, 25, and less than 5 eV, respectively. As we penetrated toward the inner torus the suprathermal fraction of the density becomes as small as 0.02% of the total density, whereas in the outer torus this fraction can be upwards of 8% by number. The partial pressures from the suprathermal electrons start to be very important in the temperate torus, and they are decidedly influential in the outer torus with the mean energy in the example shown near 120 eV, while the thermal electrons only have a characteristic energy of 30 eV. The microstate of the electrons in the torus dictates that collisional ionization rates and recombination rates should be estimated in the future by direct convolution of the measured electron distribution functions with the experimental cross sections. We can however indicate that the mean thermal energy of the

directly observed electrons is generally comparable or exceeds the
ionization thresholds of the EUV species that have beeen identified
(Broadfoot et al. (1979); Sandel et al. (1979)). Four comparisons of the
in situ properties of the electrons with indirect inferences of the
electron properties have been shown to be in excellent quantitative
agreement.

Acknowledgments

REFERENCES

Angerami, J. J. and J. O. Thomas, Studies of planetary atmospheres 1. The distribution of electrons and ions in the Earth's exosphere, J. Geophys. Res., 69, 4537, 1964.

Ashour-Abdalla, M., C. F. Kennel, and W. Livesey, A parametric study of electron multiharmonic instabilities in the magnetosphere, J. Geophys. Res., 84, 6540, 1979.

Bagenal, F., J. D. Sullivan, G. L. Siscoe, Spatial distribution of plasma in the Io torus, Geophys. Res. Lett., 7, 41, 1980.

Barbosa, D. D., D. A. Gurnett, W. S. Kurth, and F. L. Scarf, Structure and properties of Jupiter's magnetoplasmadisc, Geophys. Res. Lett., 6, 785, 1979.

Belcher, J. W., C. K. Goertz, and H. S. Bridge, The low energy plasma in the Jovian magnetosphere, Geophys. Res. Lett., 7, 17, 1980.

Binsack, J. H., Plasma studies with the IMP-2 satellite, Ph.D. Thesis, MIT, Cambridge, MA, August 1966.

Birmingham, T. J., J. K. Alexander, M. D. Desch, R. F. Hubbard, and B. M. Pederson, Observations of electron gyroharmonic waves and the structure of the Io torus, Special Voyager issue, 1981.

Bridge, H. S., J. W. Belcher, R. J. Butler, A. J. Lazarus, A. M. Mavretic, J. D. Sullivan, G. L. Siscoe, V. M. Vasyliunas, The plasma experiment on the 1977 Voyager Mission, Space Sci. Rev., 21, 259, 1977.

Bridge, H. S., J. W. Belcher, A. J. Lazarus, J. D. Sullivan, R. L. McNutt, F. Bagenal, J. D. Scudder, E C. Sittler, G. L. Siscoe, V. M. Vasyliunas, C. K. Goertz, and C. M. Yeates, Plasma observations near Jupiter: Initial results from Voyager 1, Science, 204, 987, 1979a.

Bridge, H. S., J. W. Belcher, A. J. Lazarus, J. D. Sullivan, F. Bangenal,

R. L. McNutt, Jr., K. W. Ogilvie, J. D. Scudder, E. C. Sittler, Jr., V. M. Vasyliunas, and C. K. Goertz, Plasma observations near Jupiter: Initial results from Voyager 2, Science, 206, 972, 1979b.

Broadfoot, A. L., J. J. S. Belton, P. Z. Takacs, B. R. Sandel, D. E Shemansky, J. B. Holberg, J. M. Ajello, S. K. Atreya, T. M. Donahue, H. W. Moos, J. L. Borteux, J. E. Blcmont, D. F. Strobel, J. C. McConnell, A. Dalgaeno, R. Goody, and M. B. McElroy, Extreme ultraviolet observations from Voyager 1 encounter with Jupiter, Science, 204, 979, 1979.

Broadfoot, A. L., B. R. Sandel, D. E. Shemansky, J. C. McConnell, G. R. Smith, J. B. Holberg, S. K. Atrega, T. M. Donahue, D. F. Strobel, and J. L. Bertraux, Overview of the Voyager ultraviolet spectrometry results through Jupiter encounter, J. Geophys. Res., Voyager special issue, 1981.

Brown, R. A., IAU Symposium No. 65, presented 1973, in Exploration of Planetary Systems, Woszczyke and Iwaniszewoka (eds.), IAU Publication, p. 527, 1974.

Brown, R. A., and F. H. Chafee, Jr., High-resolution spectra of sodium emission from Io, Astrophys. J., 187, L125, 1974.

Brown, R. A., R. M. Gooly, F. J. Murcray, and F. H. Chaffee, Jr., Further studies of line emission from Io, Astrophys. J., 200, L49, 1975.

Brown, R. A. and Y. L. Yung, Io, its atmosphere and optical emissions, in Jupiter, ed. T. Gehrels, 1102, 1976.

Brown, R. A., A model of Jupiter's sulfur nebula, Astrophys. J., 206, L179, 1976.

Bruining, H., Physics and Applications of Secondary Electron Emission, McGraw-Hill, 1954.

Carbary, J. F., T. W. Hill, and A. J. Dessler, Planetary spin period
acceleration of particles in the Jovian magnetosphere, J. Geophys.
Res., 81, 29, 5189, 1976.

Carlson, R. W., and D. L. Judge, Pioneer 10 ultraviolet photometer
observations at Jupiter encounter, J. Geophys. Res., 79, 3623, 1974.

Carlson, R. W., D. L. Matson, and T. V. Johnson, Electron impact ionization
of Io's sodium emission cloud, Geophys. Res. Lett.,2, 469, 1975.

Chen, C. K., Topics in planetary plasmaspheres, Ph.D. Thesis, University of
California, Los Angeles, 1977.

Cheng, A. F., Effects of Io's volcanoes on the plasma torus and Jupiter's
magnetosphere, Ap. J., 1980.

Coroniti, F. V., F. L. Scarf, C. F. Kennel, W. S. Kurth, and D. A. Gurnett,
Detection of Jovian whistler mode chorus; implications for the Io torus
aurora, Geophys. Res. Lett., 7, 45, 1980.

Cummings, W. D., A. J. Dessler, and T. W. Hill, Latitudinal oscillations of
plasma within the Io torus, J. Geophys. Res., 85, 2108, 1980.

Eshleman, V. R., G. L. Tyler, G. E. Wood, G. F. Lindel, J. D. Anderson, G.
S. Levy, and T. A. Croft, Radio science with Voyager at Jupiter:
Initial Voyager 2 results and Voyager 1 measure of the Io torus,
Science, 206, 959, 1979.

Eviatar, A., Y. Mekler, F. V. Coroniti, Jovian sodium plasma, Ap. J., 205,
622, 1976.

Fillius, R. W. and C. E. McIlwain, Measurements of the Jovian radiation
belts, J. Geophys. Res., 79, 3589, 1974.

Fillius, R. W., C. E. McIlwain, and A. Mogro-Campero, Radiation belts of
Jupiter: A second look, Science, 188, 465, 1975.

Frank, L. A., K. L. Ackerson, J. H. Wolfe, and J. D. Mihalov, Observations

of plasmas in the Jovian magnetosphere, J. Geophys. Res., 81, 457, 1976.

Goertz, C. K., Plasma in the Jovian Magnetosphere, J. Geophys. Res., 81, 2007, 1976a.

Goertz, C. K., The current sheet in Jupiter's magnetosphere, J. Geophys. Res., 81, 3368, 1976b

Gold, T. Motions in the magnetosphere of the earth, J. Geophys. Res., 64, 1219, 1959.

Grard, R. J. L., S. E. DeForest, E. C. Whipple, Jr., Comment on low energy electron measurements in the Jovian magnetosphere, Geophys. Res. Lett., 4, 247, 1977.

Gurnett, D. A., W. S. Kurth, and F. L. Scarf, Plasma wave observations near Jupiter: Initial results from Voyager 2, Science, 206, 987, 1979.

Gurnett, D. A., F. L. Scarf, W. S. Kurth, and R. L. Poynter, Determination of Jupiter's electron density profile from plasma wave observations, J. Geophys. Res., Voyager special issue, 1981.

Heald, M. A., and C. B. Wharton, Plasma Diagnostics and Microwaves, J. Wiley, New York, 1965.

Hill, T. W., Interchange stability of rapid rotating magnetosphere, Planetary Space Sci., 151, 1976.

Hill, T. W., A. J. Dessler, and F. C. Michel, Configuration of the Jovian magnetosphere, Geophys. Res. Lett., 1, 1, 3, 1974.

Hill, T. W., and F. C. Michel, Heavy ions from the Galilean satellites and the centrifugal distortion of the Jovian magnetosphere, J. Geophys. Res., 81, 4561, 1976.

Intriligator, D. S., and J. H. Wolfe, Initial observations of plasma electrons from the Pioneer 10 flyby of Jupiter, Geophys. Res. Lett.,

<u>1</u>, 281, 1974.

Intriligator, D. S., and J. H. Wolfe, Results of the Plasma analyzer experiment on Pioneers 10 and 11, in Jupiter, 848, 1976.

Intriligator, D. S., and J. H. Wolfe, Plasma electron measurements in the outer Jovian magnetosphere, <u>Geophys. Res. Lett.</u>, <u>4</u>, 249, 1977.

Ioannidis, G., and N. Brice, Plasma densities in the Jovian magnetosphere: Plasma slingshot or Maxwell demon?, <u>Icarus</u>, <u>14</u>, 360, 1971.

Jeffrey, A., and T. Taniuti, <u>Non-linear Wave Propagation with Applications to Physics and Magnetohydrodynamics</u>, Academic Press, New York, 1964.

Lepping, R. P., L. F. Burlaga, L. W. Klein, J. M. Jessen, and C. C. Goodrich, Observations of the magnetic field and plasma flow in Jupiter's magnetosheath, Voyager Special Issue, <u>J. Geophys. Res.</u>, 1981.

Kaiser, M. L., and M. Desch, Narrow band Jovian kilometric radiation: A new component, <u>Geophys. Res. Lett.</u>, <u>7</u>, 389, 1980.

Krimigis, S. M., T. P. Armstrong, W. J. Axford, C. O. Bostrom, C. Y. Fan, G. Gloeckler, L. J. Lanzerotti, E. P. Keath, R. D. Zwickl, J. F., Carbary, and P. C. Hamilton, Low-energy charged particle environment at Jupiter: A first look, <u>Science</u>, <u>204</u>, 998, 1979a.

Krimigis, S. M., T. P. Armstrong, W. I. Axford, C. O. Bostrom, C. Y. Fon, G. Gloeckler, L. J. Lanzerotti, E. P. Keath, R. D. Zwickl, J. F. Carbary, and O. C. Hamilton, Hot plasma environment at Jupiter: Voyager 2 results, <u>Science</u>, <u>206</u>, 977, 1979b.

Kupo, I., Y. Mekler, and A. Eviatar, Detection of ionized sulfur in the Jovian magnetosphere, <u>Astrophys. J.</u>, <u>205</u>, 151, 1976.

Kurth, W. S., D. D. Barbosa, D. A. Gurnett, and F. L. Scarf, Electrostatic waves in the Jovian magnetosphere, <u>Geophys. Res. Lett.</u>, <u>7</u>, 57, 1980.

McKibben, R. B., and J. A. Simpson, Evidence from charged particle studies

for the distortion of the Jovian magnetosphere, J. Geophys. Res., 79, 3545, 1974.

McNutt, R. L., Jr., J. W. Belcher, J. D. Sullivan, r. Bagenal, and H. S. Bridge, Departures from rigid co-rotation of plasma in Jupiter's dayside magnetosphere, Nature, 280, 803, 1979.

McNutt, R. L., Jr., J. W. Belcher, and H. S. Bridge, Properties of low energy positive ions in the middle magnetosphere of Jupiter, J. Geophys. Res., Voyager special issue, 1981.

Mekler, Y., A. Eviatar, and I. Kupo, Jovian sulfur nebula, J. Geophys. Res., 82, 2809, 1977.

Mekler, Y., and A. Eviatar, Thermal electron density in the Jovian magnetosphere, J. Geophys. Res., 83, 5679, 1978.

Mekler, Y., and A. Eviatar, Time analysis of volcanic activity on Io by means of plasma observations, J. Geophys. Res., 85, 1307, 1980.

Mendis, D. A., and W. I. Axford, Satellites and magnetospheres of the outer planet, Rev. Earth Planet. Sci., 2, 419, 1974.

Menietti, J. D., and D. A. Gurnett, Whistler propagation in the Jovian magnetosphere, Geophys. Res. Lett., 7, 49, 1980.

Montgomery, M. D., J. R. Asbridge, and S. J. Bame, Vela 4 plasma observations near the Earth's bow shock, J. Geophys. Res., 75, 1217, 1970.

Morabito, L. A., S. P. Synnott, P. N. Kaupferman, and S. A. Collins, Discovery of currenntly active extraterrestrial volcanism, Science, 204, 972, 1979.

Murcray, F. J., and R. M. Goody, Pictures of the Io sodium cloud, Ap. J., 226, 327, 1978.

Ness, N. F., M. H. Acuna, R. P. Lepping, L. F. Burlaga, K. W. Behannon, F.

M. Neubauer, Magnetic field studies at Jupiter by Voyager 1: Preliminary results, *Science*, *204*, 982, 1979a.

Ness, N. F., M. H. Acuna, R. P. Lepping, L. F. Burlaga, K. W. Behannon, F. M. Neubauer, Magnetic field studies at Jupiter by Voyager 2: Preliminary results, *Science*, *206*, 966, 1979b.

Neugebauer, M., and A. Eviatar, An alternative interpretation of Jupiter's "plasmapause", *Geophys. Res. Lett.*, *3*, 708, 1976.

Ogilvie, K. W., and J. D. Scudder, First results from the six-axis electron spectrometer on ISEE-1, *Space Sci. Rev.*, *23*, 123, 1979.

Pannekoek, A., Ionization in stellar atmospheres, *Bull. Astron. Inst. Neth.*, *1*, 107, 1922.

Reasoner, D. L., and W. J. Burke, Characteristics of the lunar photoelectron layer in the geomagnetic tail, *J. Geophys. Res.*, *77*, 6671, 1972.

Sandel, B. R., D. E. Shemansky, A. L. Broadfoot, J. L. Bertaux, J. E. Blamont, M. J. S. Belton, J. M. Ajello, J. B. Holberg, S. K. Atreya, T. M. Donahue, H. W. Moos, D. F. Strobel, J. C. McConnell, A. Dalgarno, R. Goody, M. B. McElroy, P. Z. Takacs, Extreme ultraviolet observations from Voyager 2 encounter with Jupiter, *Sciencce*, *206*, 962, 1979.

Scarf, F. L., D. A. Gurnett, and W. S. Kurth, Jupiter plasma wave observations: An initial Voyager 1 overview, *Science*, *204*, 991, 1979.

Scudder, J. D., and S. Olbert, A theory of local and global processes which affect solar wind electrons, 1. Steady state theory, *J. Geophys. Res.*, *84*, 2755, 1979a.

Scudder, J. D. and S. Olbert, A theory of local and global processes which affect solar wind electrons, II: Experimental support, *J. Geophys. Res.*, *84*, 6603, 1979b.

Shemansky, D. E., Radioactive cooling efficiencies and predicted spectra of species of the Io plasma torus, Astrophys. J., 236, 1043, 1980.

Simpson, J. A., D. C. Hamilton, R. B. McKibben, A. Mogro-Campero, K. R. Pyle, and A. J. Tuzzolino, The protons and electrons trapped in the Jovian dipole magnetic field region and their interaction with Io, J. Geophys. Res., 79, 3522, 1974.

Simpson, J. A., D. C. Hamilton, G. A. Lentz, R. B. McKibben, M. Perkins, K. R. Pyle, A. J. Tuzzolino, and J. J. O'Gallagher, Jupiter revisited: First results from the University of Chicago charged particle experiment on Pioneer 11, Science, 188, 455, 1975.

Siscoe, G. L., On the equatorial confinement and velocity space distribution of satellite ions in Jupiter's magnetosphere, J. Geophys. Res., 82, 1641, 1977.

Siscoe, G. L. and C. K. Chen, Io: A source for Jupiter's inner plasmasphere, (preprint 1976), Icarus, 31, 1, 1977.

Sittler, E. C., Jr., Study of the electron component of the solar wind and magnetospheric plasma, Ph.D. Dissertation, MIT, February 1978.

Sittler, E. C., Jr., J. D. Scudder, and J. Jessen, Radial variation of solar wind thermal electrons between 1.36 and 2.25 AU: Voyager 2, in Solar Wind 4 Proceedings, Burghausen, Federal Republic of Germany, H. Rosenbauer, ed., Springer-Verlag (in press), 1979.

Sittler, E. C., Jr., and J. D. Scudder, An empirical polytrope law for solar wind thermal electrons between 0.45 and 4.76 AU: Voyager 2 and Mariner 10, J. Geophys. Res., 85, August, 1980.

Sittler, E. C., Jr., and J. D. Scudder, Voyager electron results in the interplanetary medium between 1.36 and 5 AU, in preparation, 1981.

Smyth, W. H., and M. B. McElroy, Io's sodium cloud: Comparison of models

and two-dimensional images, Astrophys. J., 226, 336, 1978.

Sonnerup, B. U. O., and M. J. Laird, On magnetic interchange instability, J. Geophys. Res., 68, 131, 1963.

Strobel, D. F., and J. Davis, Properties of the Io plasma torus inferred from Voyager EUV data, Ap. J. Letters, in press, 1980.

Sullivan, J. D., and F. Bagenal, In situ identification of various ionic species in Jupiter's magnetosphere, Nature, 280, 798, 1979.

Trafton, L., T. Parkinson, and W. Macy, Jr., The spatial extent of sodium emission around Io, Astrophys. J., 190, L85, 1974.

Trafton, L., and W. Macy, Jr., An oscillating asymmetry to Io's sodium emission cloud, Astrophys. J., 202, L155, 1975.

Trafton, L., Periodic variations in Io's sodium and potassium clouds, Astrophys. J., 215, 960, 1977.

Trainor, J. H., F. B. McDonald, B. J. Teegarden, W. R Webber, and E. C. Roelof, Energetic particles with Jovian magnetosphere, J. Geophys. Res., 79, 3600, 1974.

Trainor, J. H., F. B. McDonald, D. E. Stilwell, B. J. Teegarden, and W. R., Webber, Jovian protons and electrons: Pioneer 11, Science, 188, 462, 1975.

Van Allen, J. A., D. N. Baker, B. A. Randall, M. F. Thomsen, D. D. Sentmann, and H R. Flindt, Energetic electrons in the magnetosphere of Jupiter, Science, 183, 309, 1974a.

Van Allen, J. A. D. N. Baker, B. A. Randall, and D. D. Sentman, The magnetosphere of Jupiter as observed with Pioneer 10, 1. Instrument and principal findings, J. Geophys. Res., 79, 3559, 1974b.

Van Allen, J. A., B. A. Randall, D. N. Baker, C. K. Goertz, D. D. Sentman, M. F. Thomsen, and H. R. Flindt, Pioneer 11 observations of energetic

particles in the Jovian magnetosphere, Science, 188, 459, 1975.

Vogt, R. E., W. R. Cook, A. C. Cummings, T. L. Garrard, N. Gehrels, E. C. Stone, J. H. Trainor, A. W. Schardt, T. Conlon, N. Lai, F. B. McDonald, Voyager 1: Energetic ions and electrons in the Jovian magnetosphere, Science, 204, 1003, 1979.

Warwick, J. W., J. B. Pierce, A. C. Riddle, J. K. Alexander, M. D. Desch, M. L. Kaiser, J. R. Thieman, T. D. Corr, S. Gulkis, A. Boischot, G. C. Harvey, and P. M. Pedersen, Voyager 1 planetary radio astronomy observations near Jupiter, Science, 204, 995, 1979a.

Warwick, J. W., J. B. Pierce, A. C. Riddle, J. K. Alexander, M. D. Desch, M. L. Kaiser, J. R. Thieman, T. D. Carr, S. Gulkis, A. Boischot, T. Leblanc, B. M. Pederson, and D. H. Staelin, Planetary radio astronomy observations from Voyager 2 near Jupiter, Science, 206, 991, 1979b.

Young, T. S. T., J. D. Callen, and J. E. McCune, High-frequency electrostatic waves in the magnetosphere, J. Geophys. Res., 78, 1082, 1973.

Zwan, B. T., and R. A. Wolf, Depletion of solar wind plasma near a planetary boundary, J. Geophys. Res., 81, 1636, 1976.

FIGURE CAPTIONS

FIGURE 1   Empirical relation between the plasma return current striking

the spacecraft (normalized to 1 AU) and the spacecraft

potential. (Errors of mean are in all cases smaller than

characters plotted.) This relation was derived from an

extensive analysis of Voyager 2 PLS electron measurements

taken during the cruise phase of the mission between 1.36 AU

and 4.70 AU. Data points above one volt are well represented

by a power law with negative slope. Best fit line computed

using method discussed in Sittler and Scudder (1980).

Saturation current shown dashed was estimated using charge

neutrality condition and the PLS positive ion charge density

at 64:06:39 within Io's torus when the spacecraft went

negative.

FIGURE 2   Scatter plot comparing PLS electron density determinations n-

computed at GSFC (ordinate) with the PWS broadband continuum

cutoff determinations of the electron density n_- by Gurnett

et al. (1981) (abscissa) and the PLS postive ion charge

densities n_+ by McNutt and Belcher (1981) (abscissa). The

PLS n_-, PWS n_- comparisons are indicated by the $\Diamond$ symbol,

while the PLS n_-, PLS n_+ comparisons by the + symbol. The

slope one line has been drawn for reference.

FIGURE 3   Times series day plot of electron parameters computed from

Voyager 1 PLS electron measurements on March 1, 1979 (DOY 60)

when the spacecraft crossed Jupiter's bow shock,

magnetopause, and boundary layer. In the top panel the

nearly model independent total electron number density n_e and

electron temperature T_e are displayed. The same vertical scale is used for both n_e and T_e where cgs units are used for n_e and electron volts (eV) for T_e. The spacecraft potential Φ_{SC} in volts is given in the lower panel. Solar wind, magnetosheath, and magnetosphere regimes are indicated.

FIGURE 4   The electron distribution functions f_e measured before (magnetosheath), during (boundary layer), and after (magnetosphere) the Voyager 1 crossing of the boundary layer around 20 hrs SCET on March 9, 1979, are plotted versus electron speed. For reference, the corresponding electron energy in electron volts (eV) is denoted at the top of the figure. The dashed line indicates the instrument noise level which for the high energy mode ((E2): above 140 eV) is more than an order of magnitude lower than that for the low energy mode ((E1): below 140 eV) since the speed windows are much narrower there.

FIGURE 5   Time series day plot of Voyager (inbound) PLS electron (MIT-GSFC) and magnetic field (GSFC) parameters on July 7, 1979 (DOY 188) when the spacecraft is within Jupiter's outer magnetosphere between 46 R_J and 33 R_J from Jupiter. The top panel is similar to that in Figure 3 except the symbol x has been used to explicitly show the PLS electron data points. In addition, the PWS broadband continuum cutoff determinations of the electron density by Gurnett et al. (1981) are indicated by the symbol I (see text for details). In the next panel down the tilted dipole magnetic latitude of the spacecraft λ_m in degrees has been added for reference,

where the dashed horizontal line indicates when the spacecraft passed the dipole magnetic equator (a $9.6°$ tilt angle and $202°$ system III longitude for the dipole axis was used, Ness et al. (1979a)). As in Figure 3 the spacecraft potential ϕ_{SC} is plotted but with an expanded scale. In the lower four panels the GSFC determined 48s averages of the magnetic field strength B, RTN longitude λ and latitude δ (both in degrees), and Pythagorean mean rms are plotted. The symbols N and S are used to denote whether the spacecraft is north or south of the magnetic equator as defined by the magnetometer measurements.

FIGURE 6   Voyager 1 inbound plasma sheet crossing on March 4, 1979 (DOY 63) when the spacecraft is about $16.9\ R_J$ from Jupiter. In the top panel the total electron number density n_e and suprathermal (hot component) electron number density n_h are plotted. The arrows denote the times the electron distribution functions plotted in Figure 7 were measured. In the next panel down the temperature of the suprathermal electrons T_H, total electron temperature T_e, and temperature of the thermal electrons (cold component) T_c are illustrated (see text for details). In the lower four panels the GSFC 48s averaged magnetic field parameters are given using the same format as in Figure 5.

FIGURE 7   Electron distribution functions measured during the Voyager 1 plasma sheet crossing illustrated in Figure 6 are shown. The arrows in Figure 6 denote the times sampled. The same format is used, as in Figure 4 where the Gaussian fits to the cold

component have been indicated by the dashed lines, while the noise level trace has been omitted.

FIGURE 8   Voyager 2 outbound plasma sheet crossing on July 10, 1979, (DOY 191) when the spacecraft is about 13 R_J from Jupiter. The same format as Figure 6 is used.

FIGURE 9   Electron distribution functions measured during the Voyager 2 plasma sheet crossing illustrated in Figure 8 are shown. The same format as Figure 7 is used.

FIGURE 10   In each panel the electron distribution function measured at different times within Io's plasma torus by the Voyager 1 PLS experiment are plotted. The measurement times, radial distance of spacecraft from Jupiter, system III longitude of spacecraft relative to Io, and dipole magnetic latitude of the spacecraft are indicated. For each panel the same format used in Figures 7 and 9 are used where in addition the computed electron parameters are given (see text for details). Horizontal (energy) uncertainties in Figure 10c reflect the available, though imprecise, knowledge of the spacecraft potential at this position. When the observational limits on the potential are refined new estimates of the effective spread of thermal speeds below 10 eV will be made. If $T_c \sim 5$ eV (determined from data immediately above 10 eV) correctly parameterizes $f(\underline{v})$ below 10 eV, as currently assumed, then the spacecraft must be -12 volts with respect to the plasma. If external measurements require $\phi \sim 0$ V then an even colder component below 10 eV must be present with temperature T_c less than 1.7 eV.

PLASMA RETURN CURRENT RELATION   (GSFC-MIT)

VOYAGER 2
POWER LAW FIT
SLOPE = -2.0 ± 0.08
INTERCEPT = -5.1 ± 0.02
5785 HOURLY AVG.
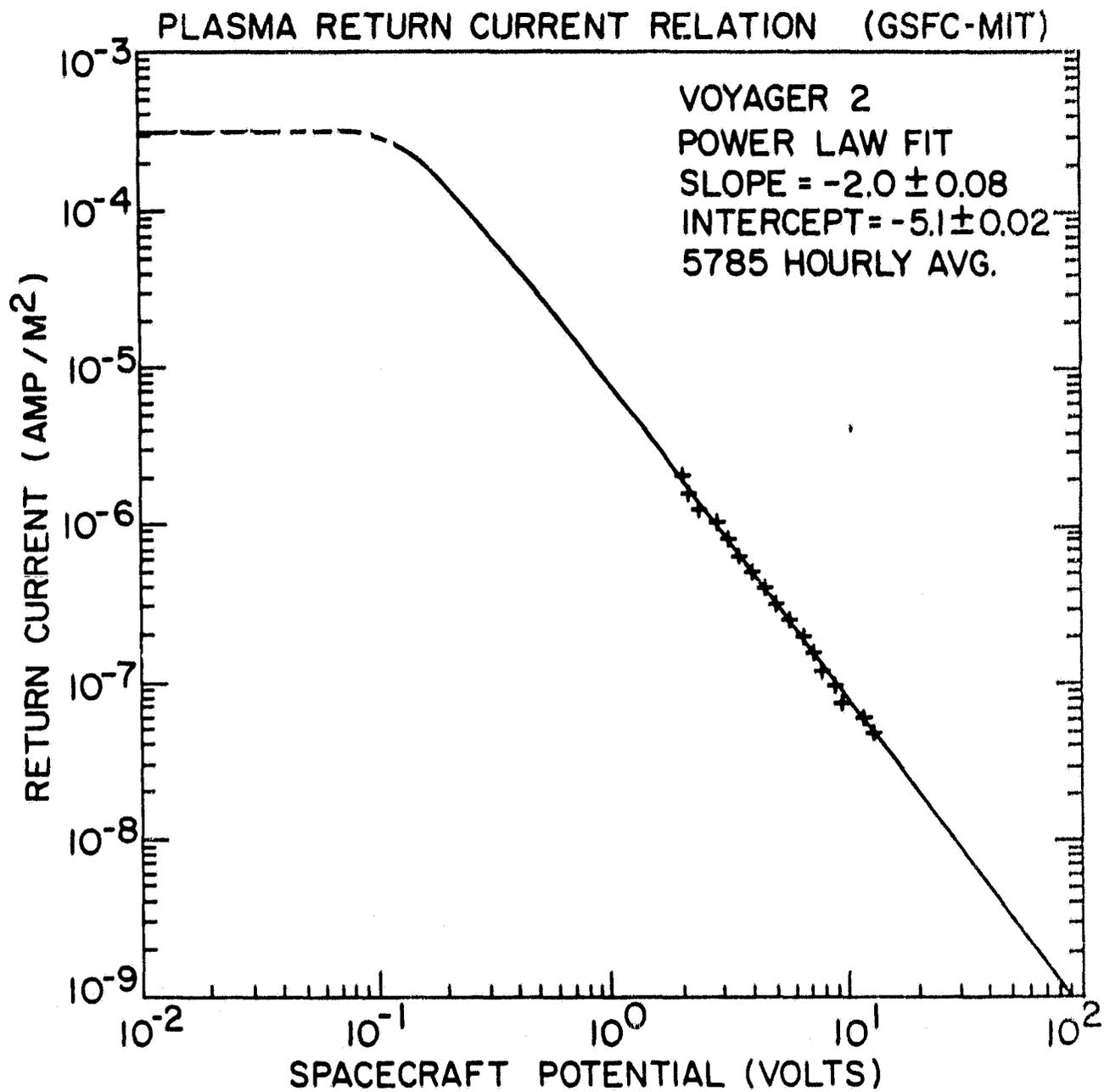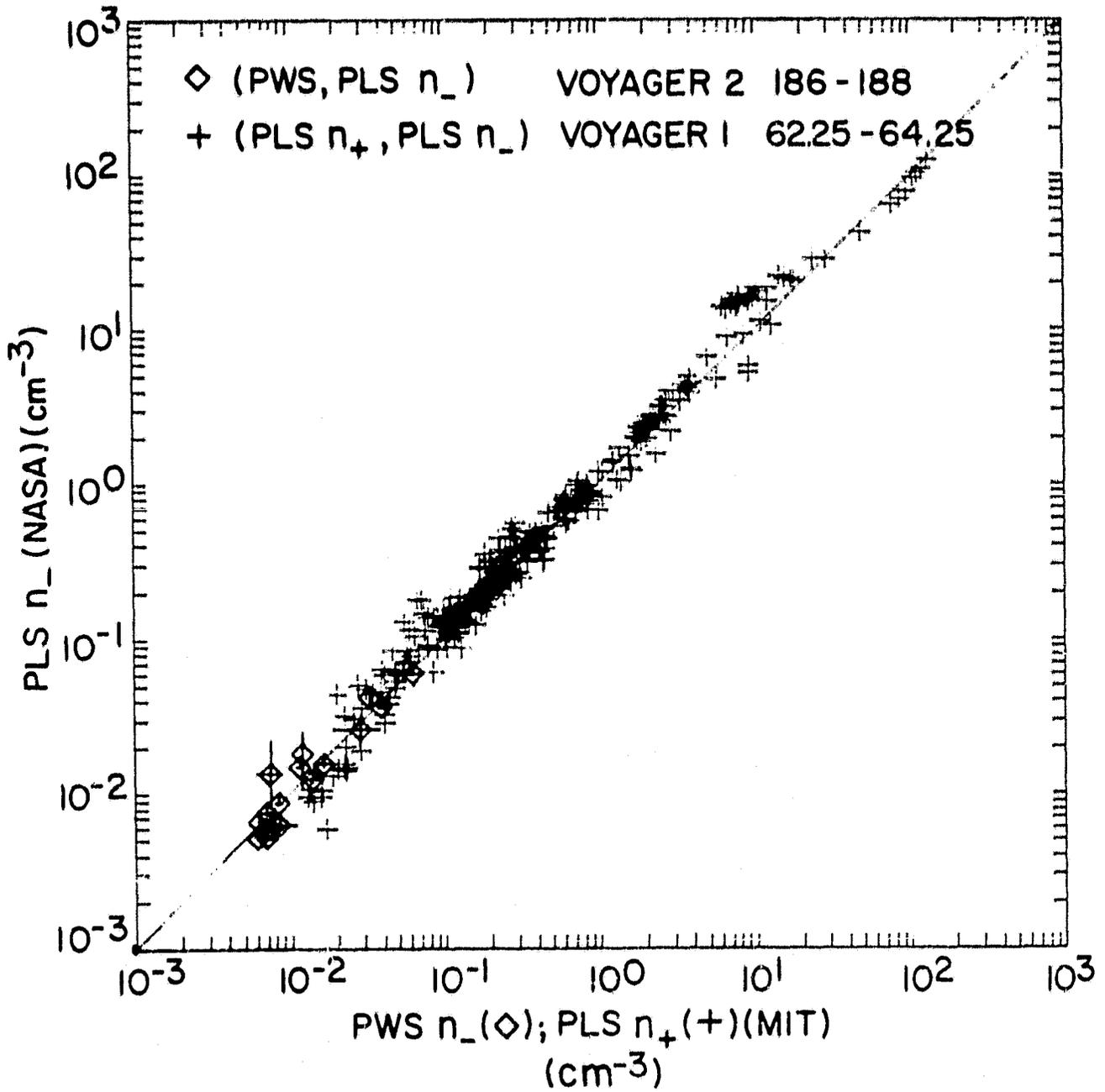
Figure 1

Figure 2

VOYAGER 1 PLS ELECTRONS GSFC/MIT

MAGNETOSPHERE

MAGNETOSHEATH

SOLAR WIND

$T_e(eV)$

$n_e(/cc)$

$\Phi_{SC}(VOLTS)$

MARCH 1, 1979 (DOY 60)

Figure 3

VOYAGER I PLS
GSFC-MIT

△ 60:19:55:43
□ 60:20:02:07
○ 60:20:18:07

MARCH 1, 1979

MAGNETOSHEATH

BOUNDARY LAYER

MAGNETOSPHERE

NOISE LEVEL

E (eV)

SPEED (10^3 km/sec)
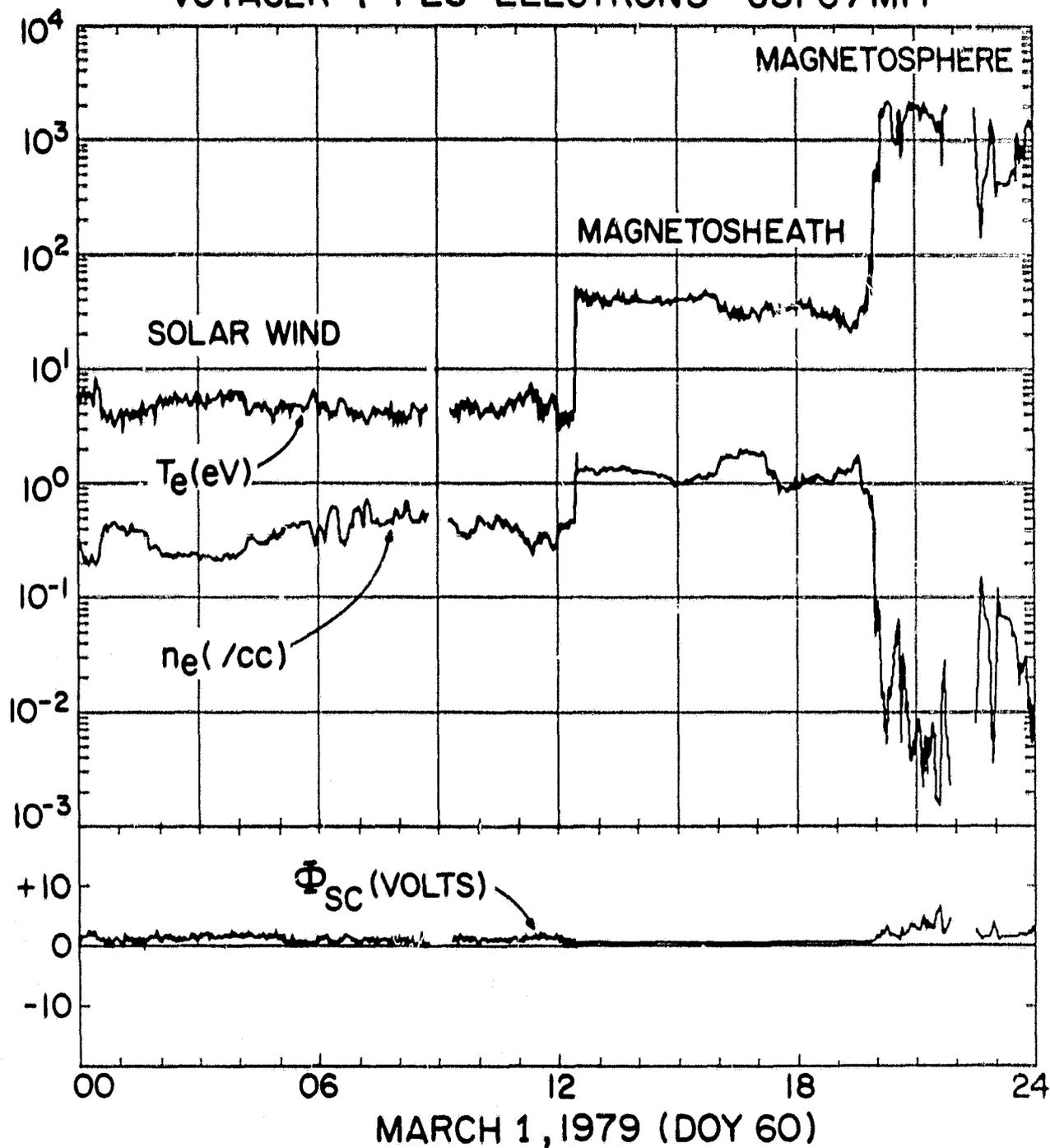
f_e (cm^{-6}sec^3)

Figure 4

VOYAGER 2 PLS ELECTRON PARAMETERS GSFC-MIT

Figure 5

VOYAGER 1 PLASMA ELECTRONS GSFC-MIT

MARCH 4, 1979 (DOY 63)
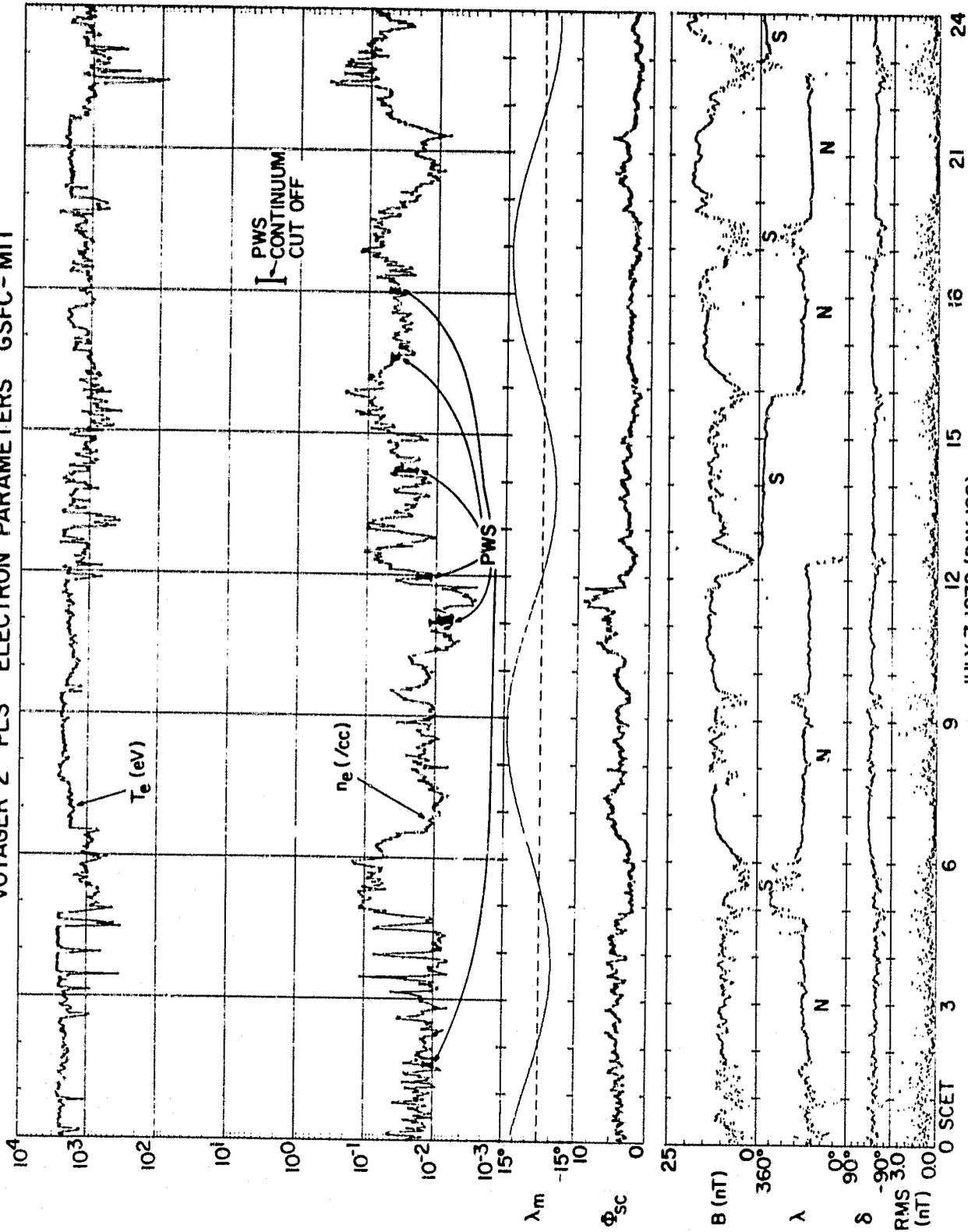
Figure 6

Figure 7

VOYAGER 2 PLASMA ELECTRONS GSFC-MIT

Figure 8

VOYGER 2 PLS ELECTRONS
GSFC-MIT

● 191 09:01:30	12.87 R_J
□ 191 09:28:42	13.04 R_J
○ 191 09:54:18	13.29 R_J

JULY 10, 1979
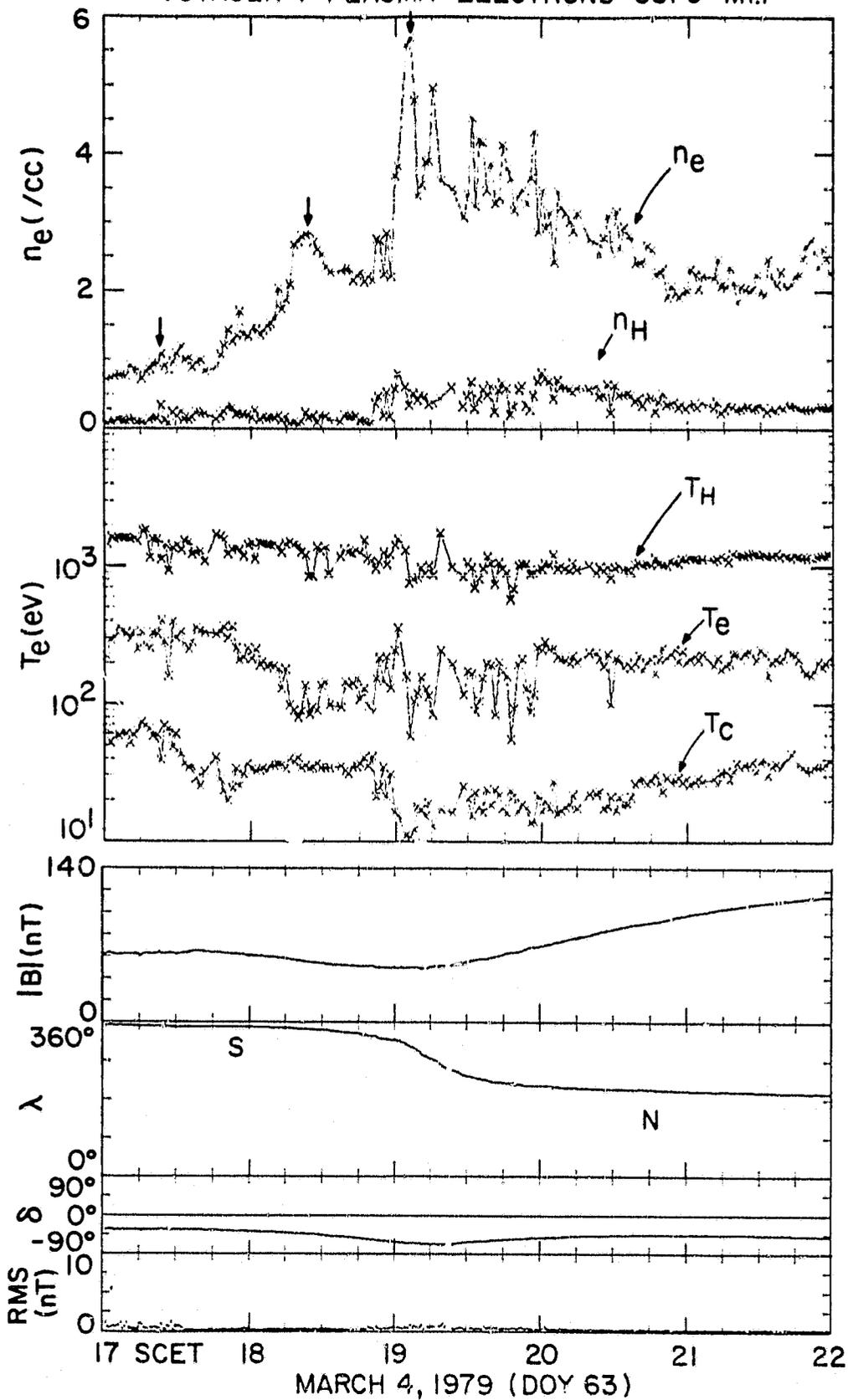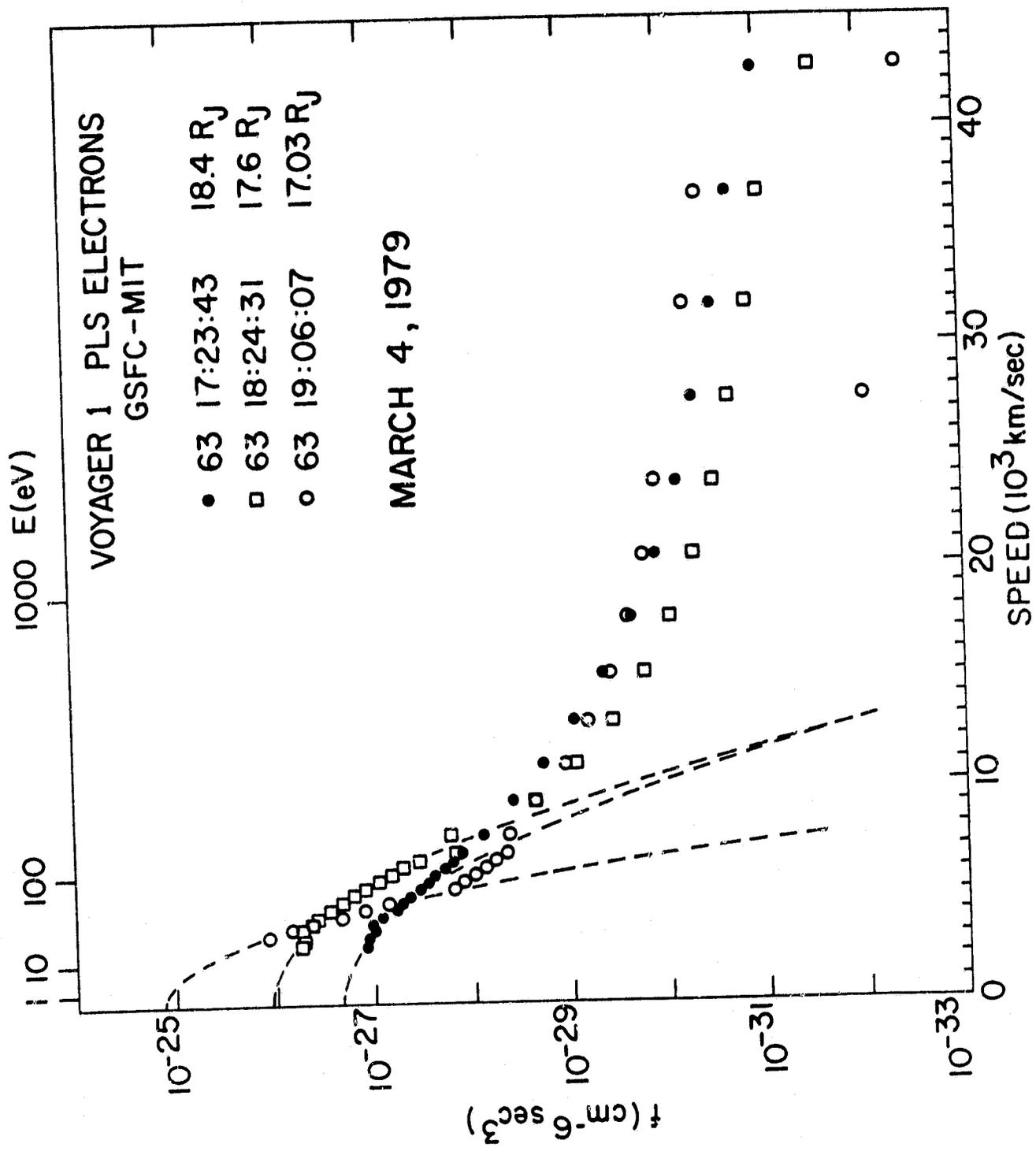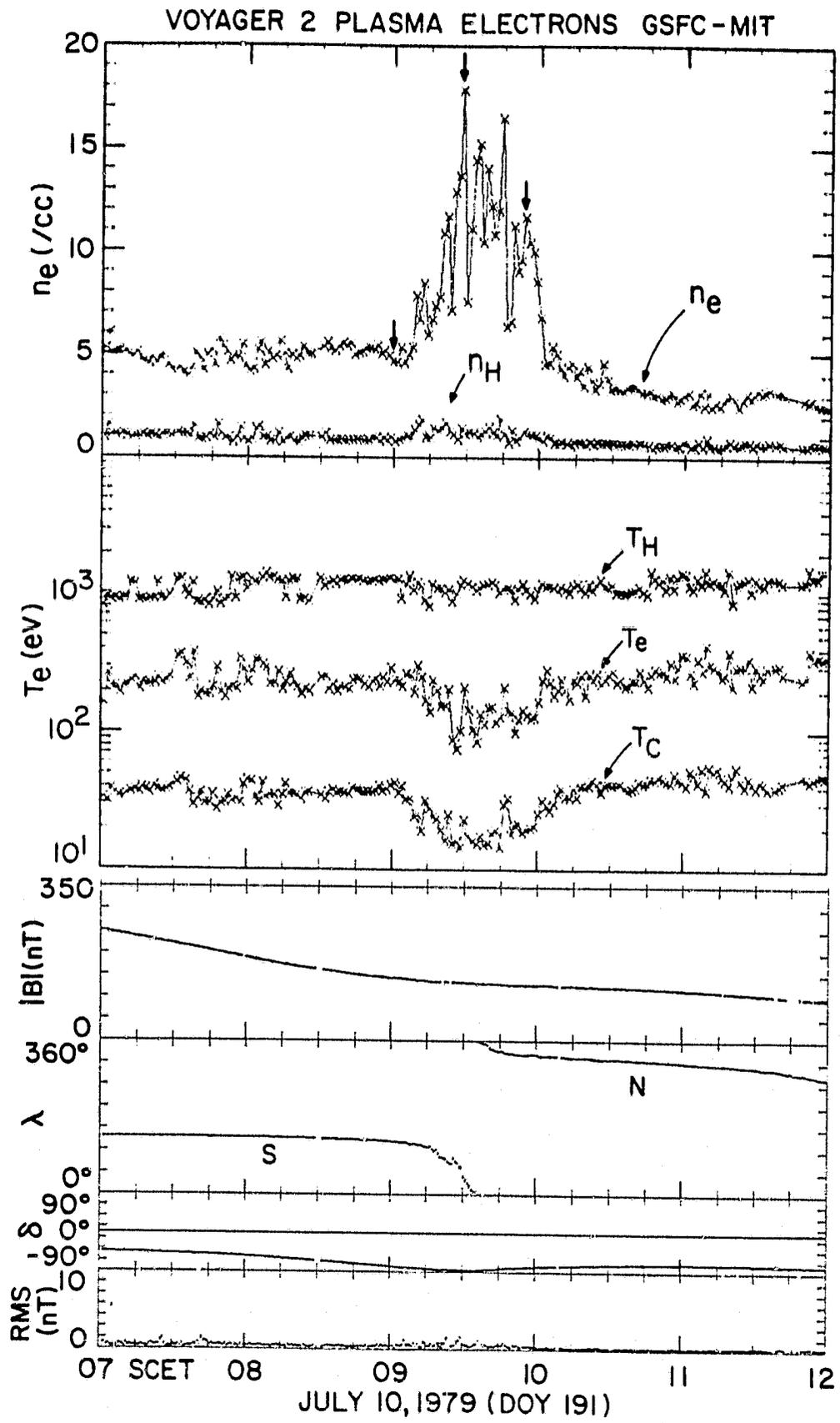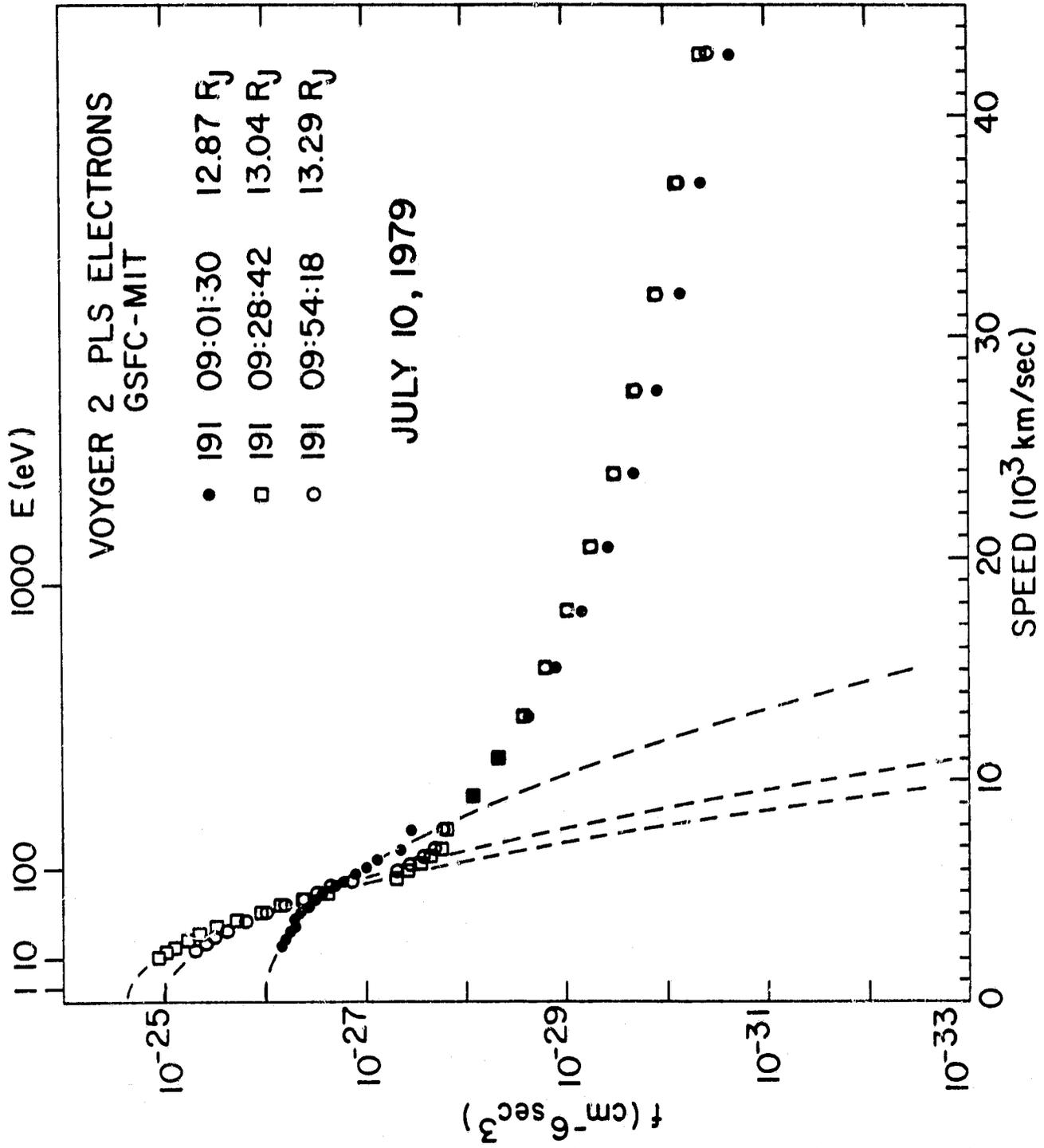
Figure 9

VOYAGER 1   PLS ELECTRONS   GSFC - MIT
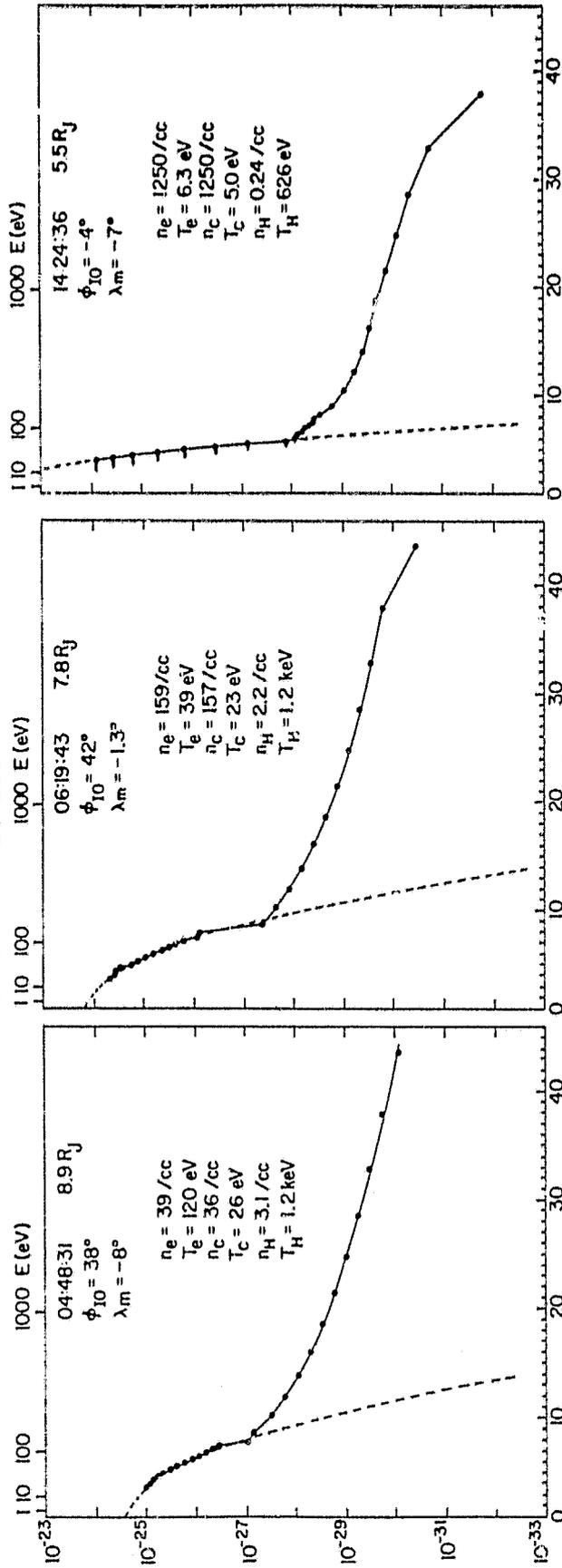
MARCH 5, 1979 (DOY 64)

Figure 10